Master Thesis

im Rahmen des Universitätslehrganges „Geographical Information Science & Systems" (UNIGIS MSc) am Interfakultären Fachbereich für GeoInformatik (Z_GIS) der Paris Lodron-Universität Salzburg

zum Thema

Assessing Shrub and Tree Encroachment in Alpine Pastures from Airborne Laser Scanning Data

vorgelegt von

Dipl. Ing. Christoph Giger
104172, UNIGIS MSc Jahrgang 2015

Zur Erlangung des Grades
„Master of Science (Geographical Information Science & Systems) – MSc(GIS)"

Gutacher:
Dr. Lars T. Waser

Bern, 31. Dezember 2017

Eigenständigkeitserklärung

Hiermit erkläre ich, dass ich die vorliegende Masterarbeit selbständig verfasst habe, dass ich sie zuvor an keiner anderen Hochschule und in keinem anderen Studiengang als Prüfungsleistung eingereicht habe und dass ich keine anderen als die angegebenen Quellen und Hilfsmittel benutzt habe. Alle Stellen der Arbeit, die wörtlich oder sinngemäss aus Veröffentlichungen oder aus anderweitigen fremden Äusserungen entnommen wurden, sind als solche kenntlich gemacht.

Bern, 31. Dezember 2017

Christoph Giger

Abstract

The forest area in the Alpine region is increasing. Agricultural land is being abandoned – shrub and tree encroachment and reforestation are the consequences. Various actors from agriculture, nature conservation and tourism assess this process as negative. The importance of alpine and mountain farming will continue to be high in the future. Experts and layperson in Switzerland reject a strong reforestation for a variety of reasons, especially in alpine pastures, which are an outstanding element of the cultural landscape of Switzerland.

Various projects have the goal of making such areas suitable for agriculture again. Adapted grazing, other livestock or initial interventions with felling of trees or rooting out bushes to keep them open in the long term.

This thesis investigates, whether with ALS data (Airborne Laser Scanning) areas of shrub and tree encroachment can be identified. Therefore, a workflow was developed using a method for the identification of such vegetation structures implemented in free and open source software. The resulting information can be visualised, analysed and prioritised – depending on the needs of the specific project.

Based on evaluations of the Swiss Land Use Statistics conducted by the Federal Statistical Office and the availability of ALS data, three study areas were selected. For these areas, data from two aerial surveys with a time difference of at least 10 years, using a point density of 0.8 to 4.2 p/m2 (2001/2002) and 9.8 to 21.7 p/m2 (2011-2015) are available.

In a 3m grid, the Vertical Complexity Index (VCI), which provides information about the vertical distribution of laser points and the maximum Z value of the vegetation per grid cell are calculated.

The results of the ALS data evaluation were compared with manually collected data from the interpretation of orthophotos. ALS data evaluation indicated that with higher point density, the detection rate for areas with shrub and tree encroachment is higher. With more than 4 points/m^2, the correspondence between the calculation of the ALS data and

the interpretation of the orthophotos is between 57 and 79 percent for the category *shrub and tree encroachment* and between 90 and 98 percent for the category *other*.

The achieved accuracies for the encroachment indicator are sufficient for the localization of encroachment. In order to identify areas of priority among potential stakeholders, the visualization and quantification of the resulting data are a solid basis.

Zusammenfassung

Die Waldfläche im Alpenraum nimmt zu. Landwirtschaftliche Nutzflächen werden aufgegeben – Verbuschung und Wiederbewaldung sind die Folgen. Verschiedene Akteure aus Landwirtschaft, Naturschutz und Tourismus beurteilen diesen Prozess negativ. Die Bedeutung der Alp- und Landwirtschaft in Bergregionen wird auch in Zukunft hoch sein. Experten und Laien in der Schweiz lehnen eine starke Wiederbewaldung aus vielfältigen Gründen ab, insbesondere die Verbuschung von Alpweiden, die ein herausragendes Element der Kulturlandschaft der Schweiz sind.

Verschiedene Projekte haben zum Ziel verbuschende oder verwaldende Flächen durch angepasste Beweidung, andere Nutztiere oder mittels Initialeingriffen wieder landwirtschaftlich nutzbar zu machen und langfristig offen zu halten.

In dieser Arbeit wird untersucht, ob mit Hilfe von ALS (Airborne Laser Scanning) Daten solche Flächen identifiziert werden können. Dazu wird mit frei verfügbarer Software ein Arbeitsablauf entwickelt und eine Methode zur Identifizierung solcher Vegetationsstrukturen eingesetzt. In der Folge können die resultierenden Informationen projektspezifisch visualisiert, analysiert und priorisiert werden.

Basierend auf Auswertungen der Arealstatik des Bundesamt für Statistik sowie der Verfügbarkeit von ALS Daten wurden drei Versuchsregionen ausgewählt. Für diese Regionen sind Daten aus zwei Befliegungen mit einem Abstand von mindestens 10 Jahren und mit einer Punkdichte von 0.8 bis 4.2 Punkten/m^2 (erster Zeitstand) und 9.8 bis 21.7 Punkten/m^2 (zweiter Zeitstand) vorhanden.

In einem 3 Meter Raster wird der Vertical Complexity Index (VCI) und der maximale Z-Wert der Vegetation pro Rasterzelle ermittelt. Mit dem VCI wird die vertikale Verteilung von Laserpunkten berechnet.

Die Resultate der Auswertung der ALS Daten wurden mit manuell erhobenen Daten aus der Interpretation von Orthophotos verglichen. In den Studiengebieten hat sich gezeigt, dass bei höherer Punktdichte der Daten die Erkennung von Flächen mit Verbuschungscharakter grösser ist. Bei mehr als vier Punkten pro m^2 liegt die

Übereinstimmung zwischen dem berechneten Indikator aus den ALS Daten und der Interpretation der Orthophotos zwischen 57 und 79 Prozent für die Kategorie *Gebüsche und Bäume* und zwischen 90 und 98 Prozent für die Kategorie *Anderes*.

Für die Lokalisierung von Verbuschungsflächen ist die aufgezeigte Genauigkeit ausreichend. Die Visualisierung und Quantifizierung der resultierenden Daten können somit für Entscheidungsträger eine Grundlage für die Priorisierung von Massnahmen bilden.

Table of Contents

List of Figures

List of Tables

Glossary

AGB   Above Ground Biomass

ALS   Airborne Laser Scanning

CHM   Canopy Height Model

DSM   Digital Surface Model

DTM   Digital Terrain Model

IDE   Integrated Development Environment

LAS   File Format for point clouds from laser scanners (LASer)

LAZ   with LASzip from LAStools compressed LAS File

LFI   Swiss National Forest Inventory

LiDAR Light Detection and Ranging

UAV   Unmanned Aerial Vehicle

VCI   Vertical Complexity Index

WSL   Swiss Federal Institute for Forest, Snow and Landscape Research

Acknowledgements

1 Introduction

1.1 Motivation

Regions with alpine pastures[1] are areas with distinguished value for biodiversity and an above-average richness of species, particularly in patches with forested areas. Zoller and Bischof (1980) summarise that alpine pastures show three times the number of species than the forest they replace. As part of the *AlpFutur* collaborative project, Koch and Schmid (2013) highlight in their study the significant influence of dwarf shrubs on decreasing of herb and grass species composition. According to Battaglini et al. (2014), the traditional use of meadows and pastures has "fundamental positive externalities and ecosystem services", such as the conservation of genetic resources, water flow regulation, climate regulation or landscape maintenance.

Seasonal alpine grazing fulfils several functions for the environment, agriculture and regional economy – around 25 % of total livestock of Switzerland (Mack et al., 2013) spends the summer on one of 7058 alpine summer farms in the mountain area (agriculture census 2013, Bundesamt für Landwirtschaft BLW, 2016). Letting cows, cattle and goats graze on summer pastures has a long tradition and formed a unique alpine landscape.

As in all mountain areas in Europe, wooded area in Switzerland is increasing due to agriculture abandonment (MacDonald et al., 2000). Particularly in regions with alpine pastures where two-thirds of encroachment areas grew between the middle of the 80ies and the middle of the 90ies. The tendency for intensification of well accessible meadows on one hand and extensification or abandonment of remote or steep meadows on the other hand has not been broken (Baur et al., 2007). In the region of alpine pastures and meadows in Switzerland forest increases by 2'400 ha per year (Lauber et al., 2013, Brändli et al., 2014).

---

[1] In this thesis the term 'alpine pasture' is used for seasonal used grazing areas in Swiss mountains, including partly mowed pastures or meadows that only are mowed and not grazed by livestock.

Impact of this spontaneous reforestation on the ecosystem function is not necessarily negative at global scale. From the view of pastoral land use encroachment of woody plants tends to have a negative impact on the asked ecosystem function grazing of grassland (Eldridge et al., 2011). Due to the regulation for direct payments (Schweizerischer Bundesrat, 2013) the area of alpine pasture has to be protected from shrub and tree encroachment (Art. 29 Abs. 1). But carrying out and controlling in practice is difficult (Agridea, 2015).

Different stakeholder have initialised projects to work against the process of reforestation. To identify areas of encroachment over a large area with remote sensing could help to assign priorities.

1.2 Objective

The objective of this thesis is to compare a method for detection of shrub and tree encroachment from ALS data in farming areas of Switzerland with manual digitized reference data from orthophotos.

The comparison shall answer the followed questions:

1. Is it possible to detect shrub and tree encroachment from ALS data with open source tools and standard available data?
2. What is the detection rate for ALS based method compared to manually digitized data?
3. What is the minimal point density of ALS data to obtain a reasonable detection rate?

1.3 Structure

Chapter 2 introduces the technology of Airborne Laser Scanning, processing of LiDAR data and gives background information about alpine pastures. The question where encroachment is present in Switzerland will be addressed in chapter 2.4. In chapter 3 criteria for selecting the study areas and the three study areas are described. Chapter 4 will explain the methodology and describe the applied LiDAR data processing workflow. In chapter 5 and 6, the results from the three study areas are presented and discussed. Finally, conclusions are drawn and potential future work is listed.

2 Background

2.1 LiDAR

Light Detection And Ranging (LiDAR) is an active optical remote sensing technique using laser light, operating in the wavelength regions from visible to infrared. From a platform (airborne, terrestrial or even satellite), laser pulses are sent out and reflected by buildings, vegetation, the ground or so called noise like birds, clouds or aerosols (Figure 1). From the return time of each pulse the distance to each object is calculated. The signal is stored as discrete return data or as full-waveform information (Lillesand et al., 2014, McGill, 2003). Airborne Laser Scanning (ALS) is often used when the data is acquired from a plane or a UAV (Unmanned Aerial Vehicle).
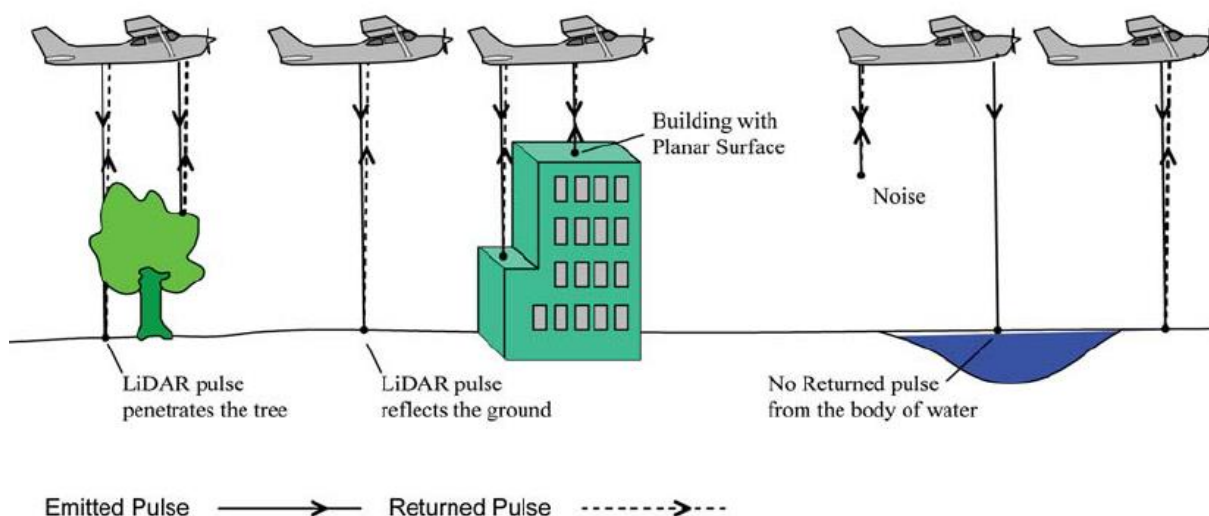
Figure 1: Acquisition of Airborne LiDAR data (source: Karan et al., 2013)

Multiple-return LiDAR systems enable to detect different vegetation layers. When the laser pulse hits an object, a part of the energy is reflected back to the receiver (first return). Figure 2 illustrates the case, where the object does not completely block the pulse. The remaining part intercepts with lower branches, trunks, shrubs or the ground. This results in up to five returns from the same laser pulse. From these multiple returns information about canopy height, forest structure or even tree species can be obtained (e.g. Hyyppä et al., 2009, Cao et al., 2016).
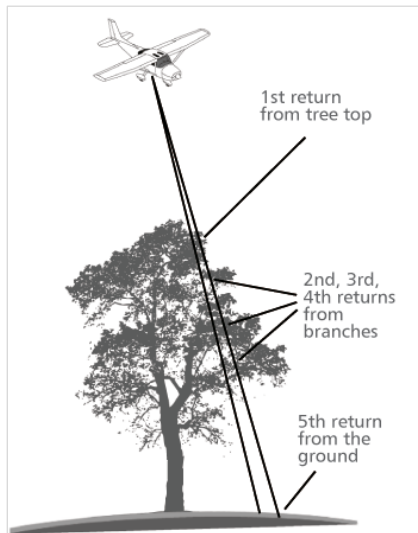
Figure 2: Multiple returns from laser pulse (source: Balenović et al., 2013)

For a wide range of applications in many fields LiDAR is used as basis for visualisation, analysis and surveying (Heipke, 2017; Caldwell, 2013). Some common products and use cases are:

- DTM, DEM, and DSM: Calculation of a digital terrain model (DTM), digital elevation-model (DEM) or digital surface- model (DSM) from LiDAR point data is very common. These products are essential for a wide range of application in the private and public sectors and divisions. In Switzerland, the Federal Office of Topography swisstopo provides a DTM with an accuracy of 2 m (Bundesamt für Landestopographie swisstopo, 2016).

- Collecting detailed forest information: Important forest structural parameters such as e.g. basal area, canopy heights, stand volume, subcanopy topography and biomass can be accurately estimated with LiDAR. This helps collecting accurate data for small to medium areas for forest planning and managing purpose or research. Furthermore, parameters, such as single tree detection or forest 3D metrics and spatial pattern can be determined. For many purposes in forestry, using LiDAR has become a standard (Ginzler and Waser, 2017; Mongus and Žalik, 2015; Blaschke et al., 2004).

- Building models and facades reconstruction (aerial and terrestrial LiDAR): Extracting accurate 3D models of buildings from LiDAR data for solar potential

(Bizjak et al., 2015) or detailed visualization for construction renovating, urban planning and security monitoring (Yang et al., 2016).

- Detection an explanation of archaeological features and sites: Large scale phenomena and showing unknown relationships in structure or arrangement hidden from forest canopies (e.g. Devereux et al., 2005).

- Dimensioning and monitoring mine dump or location of emplacement (Esposito et al., 2017).

- Detection of impact due to natural disaster and analysis for prevention: Modelling floodplains, natural coastal hazards, observation of landslides and hydrogeological risk mapping.

- Bathymetry, Underwater laser scanning (Mandlburger, 2017).

- Measurement of snow depth (Deems et al., 2013).

- Repeating LiDAR data collection in the same area in defined and reasonable time interval leads to further interesting fields of application: landscape and vegetation change or monitoring wildlife habitat.

Point Density

The density of point cloud data is important for several reason. Less density means less cost for data acquisition. For many purpose low to middle density is sufficient. In order to generate a DTM for natural disasters prevention, fewer points per square meter are needed then for detailed archaeological purpose.

According to Hellesen and Matikainen (2013) a density of 2 points/m^2 can be sufficient for the detection of individual trees. The same authors used an average point density of 13 points/m^2 for the mapping of even small shrubs and trees. For aboveground biomass (AGB) estimation, Wu et al. (2016) obtained high accuracies using 8 points/m^2.

Full-waveform LiDAR

Waveform LiDAR systems enable to measure time-varying signals of the laser pulse. Full-waveform data enable to describe the 3D structure of vegetation canopies more accurately than discrete return data, in particular the canopy understorey (Anderson et al., 2016). Even tree species can be extracted from full-waveform LiDAR for example for tree inventories (Bruggisser et al., 2017). For classifying grassland vegetation in open landscape, Alexander et al. (2015) showed advantages of full-waveform ALS over other remotely sensed data.

Full-waveform data on one hand are cost intensive regarding data processing but on the other hand enable an improved method for measuring the three-dimensional structure of vegetation systems. In the future, improved toolkits will reduce these costs and thus increase accessibility of this information for a wider range of analysis and applications.

2.2 Processing LiDAR Data

Nowadays, a wide range of free and open source and non-free software for processing LiDAR data is available. Table 1 lists software for LiDAR-processing and their functionalities. The list is not complete; it gives an overview of available software and tools found during the investigations for this thesis. Workflows and processes in R, python and toolboxes for other software or standalone solutions are listed as well.

Table 1: Software in comparison

Name	Company / Developer	Functions	Licence*
Ecognition Developer	Trimble	Filter, analysis, extraction, combining with OBIA	non-free
Fugro Viewer	Fugro	.las / .laz viewer	FTU
R	r-project	rLiDAR - 2D / 3D Convex hull of individual tree - 3D stand visualization of individual tree - Canopy Height Model (CHM) - CHM smoothing - Individual tree detection	OS AGPLv3
		lidR - read, write .las, .laz - plot / - filter (first, last, first and last, firstofmany, single, by classification) - ground (progressive morphological filter) - normalization - Canopy height model	OS GPL-3
TIFFS	Globalidar	Filter, data conversion, DEM, DSM, object height models (OHM), object extraction (individual trees, buildings)	non-free
Lastool l	Rapidlasso	laszip / lasindex / lasvalidate / lasliberate / lasinfo / las2las / lasdiff / lasmerge / las2txt & txt2las / lasprecision / LASzip (with static linking exception) / LASlib (with LASzip) - the API used by LAStools. Free but not open source: Lasview / laspublish	FTU LGPL 2.1 LASzip: OS

*OS: open source / FTU: free to use

Lastool II	Rapidlasso	blast2dem / blast2iso / lasground & lasground_new / lasheight / lastrack / lasclassify / lasgrid / lascanopy / lasboundary / lascontrol / lasoverlap / lasoverage / lasduplicate / lassplit / lasreturn las2tin / las2iso / las2dem / lasthin & lasnoise / lassort / lastile / lasplanes / lascolor / lasclip / las2shp & shp2las	non-free
ArcGIS	ESRI	3D Analyst Tools > Data Management > LAS Dataset (Change Class, Classify, Extract, Statistics, Locate, Set Class Using Features) / Conversion > LAS Dataset to TIN, LAS to Multipoint	non-free
FUSION	US Department of Agriculture	Cover.exe (Canopy Cover) Dtm2ascii.exe (export .asc for import in qgis) gridsurfacecreate.exe (average elevation perc ell) canopymodel.exe (canopy surface model)	FTU
LiForest 2.1	Greenvalley International	Point Classification Surface Models Canopy Cover Tree segmentation, tree location, crown size, tree height	free
PDAL	Hobu, Inc.	Able to manipulate data with Python	OS BSD
OPALS	Vienna University of Technology	Modular based functions for processing ALS data: georeferencing, quality check, filter, algebra, DSM	non-free
GRASS	GRASS Development Team	Import, filtering, analysing (outliers, edge detection, building contour determination) DEM, terrain change, visualization	OS GPL
SPDlib		Converting, merging, DTM, Classify ground returns, processing large datasets, vegetation metrics (HSCOI, Canopy Openness, waveform	OS
Laspy		python library for reading, modifying, and creating .las files - lascopy - lasexplorer - lasvalidate	OS BSD 2
pyLidar		Turn data in to structured arrays for further processing and working with the data directly in numpy arrays. Check, analyse data in small blocks. Based on SPDlib, built on RIOS	OS GPL-3
LibLAS		LibLAS has been almost entirely superseded by Martin Isenburg's LASlib library Conversion, links with GDAL functionality.	OS BSD

ARSF DEM scrips	Daniel Clewley	Library ('wrapper') for GRASS-tools combined with Python functions. DEM, DSM, DTM, Intensity, Density, Create mosaic from DEM, load LiDAR to GRASS	OS GPL-3
QGIS	QGIS Development Team	QGIS toolbox for LAStools. Easy way of using LAStools – depended on licence the tools from Lastool I or Lastool II (see above) are available.	QGIS: OS GPL LAStools: see above
Cloud Compare	Daniel Girardeau-Montaut	Visualizing point clouds	OS GPL
Greyhound	Hobu, Inc.	Stream and query point cloud data over network	OS Apache License 2.0
Entwine	Hobu, Inc.	Data organization library. Organisation tool for massive point cloud collection	OS LGPL
Plas.io		WebGL HTML5 point cloud renderer	OS MIT
Potree		WebGL HTML5 point cloud viewer for large datasets	OS
PCL		Standalone, large scale, open project for 2D/3D image and point cloud processing. Filtering, Segmentation, Surface reconstruction, Model fitting	OS BSD-3

2.3 Alpine Pastures: Borders and Limitations

Definition and borders of alpine pastures and meadows may differ from region to region. The regulation for zoning the agricultural used area says: "The limits of alpine pasture and meadows are defined by the management before 1999 and taking into account the conventional-traditional management" (Art. 3, Bundesamt für Landwirtschaft BLW, 2017).

A lower altitude limit for alpine pastures is clearly defined in most regions by the boundary to all season's meadows and pastures. The upper altitude limit for grazing areas differs from region to region, but in general is set by approx. 2000 m a.s.l. for the northern Pre-Alps and up to approx. 2400 m a.s.l. for the Central-Alps (McC. Netting, 1972; Mack et al., 2013; Hedinger, 2014).

In the register of agricultural production (Bundesamt für Landwirtschaft BLW, 2017) the agricultural area is divided into 1) summer pastures, 2) mountainside areas, 3) hilly areas and 4) valley areas. The mountainside areas themselves are divided into four zones. For this classification, the following criteria have to be considered due to Art. 2 of the regulation (Bundesamt für Landwirtschaft BLW, 2017):

- Climatic location, in particular the duration of the growing period
- Traffic situation and development
- Morphology and topography, in particular the proportion of hillside and steep slope

Various measures in the field of the agricultural law are based on the zoning. For example, payments for promotion of ecological network and farmland biodiversity differ between the zones.

Apart from the question of the upper and lower borders of alpine pastures, slope is another category of interest for this thesis. Whether a pasture can be grazed due its slope or not, depends primarily on cattle species and race. According to Sutter (2007) the upper limit of slope is 40% for cows, 60 % for cattle and up to 80% for sheep and goats.

2.4 Landscape Dynamic in Agriculture

The Swiss Land Use Statistics conducted by the Federal Statistical Office is based on sample points of a 100 m regular raster, in total 4.1 million (Bundesamt für Statistik BFS, 2014). The classification scheme distinguishes 72 categories, which are aggregated to 17 and 27 classes respectively. These aggregated classes are allocated to one of the four major division: 1) *settlement and urban areas*, 2) *agricultural areas*, 3) *wooded areas* and 4) *unproductive areas.* In this thesis, the change of classification from the major class *agricultural area* to *wooded area* is used as an indicator for shrub and tree encroachment. The dataset (Bundesamt für Statistik BFS, 2016) provides information about the change of land use between 1992/97 and 2004/09. All sample points that indicate a change of land use in this time are visualized in Figure 3.
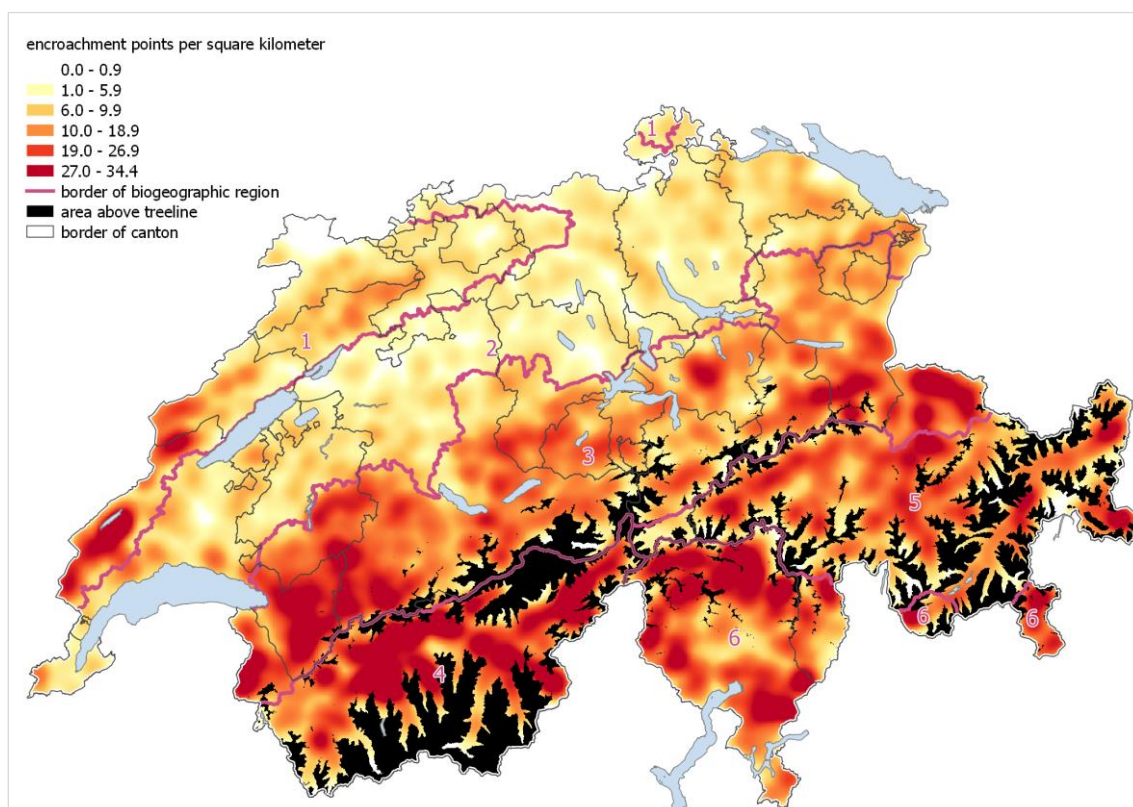
Figure 3: Change of classification agricultural areas to wooded areas (illustration by author, data: swisstopo[2], BAFU[3])

---

[2] Swiss Federal Office of Topography: swissTLM3D

[3] BAFU: Bio-geographical regions, number of biogeographic region corresponding to Figure 6

Figure 3 shows the characteristic of change of land use classification from *agricultural areas* to *wooded areas* corresponding to the biogeographic region (see chapter 3.2). The plateau region (2), which is a region of particularly intensive agriculture, is characterized by fewer changes of *agricultural areas* into *wooded areas*. Areas with a high density of encroachment points are in particular located in the southern parts of Switzerland, in the Alps and Prealps, and in the western parts of the Jura.

Table 36 (Appendix A) shows the results of landscape dynamic analyses as total encroachment points per canton and per square kilometre. The mean encroachment points per square kilometre range between 0.03 for the canton Basel-Stadt, rise up to 0.37 for the canton Valais, and 0.48 for canton Ticino.

Belt of Potential Encroachment Concentration

The border for summer pastures from the register of agricultural production as mentioned in chapter 2.3 is not digitized very accurately and includes errors such as borders around lakes, but not around settlements or forested area. Nevertheless, for analysing a potential concentration of encroachment in this area of interest, a buffer around this borderline was used in this thesis.

Overlaying the density map of encroachment points in Figure 3 with the summer pasture border, a concentration of encroachment around this border is obvious (see Figure 4, Table 2 and

Table 3).
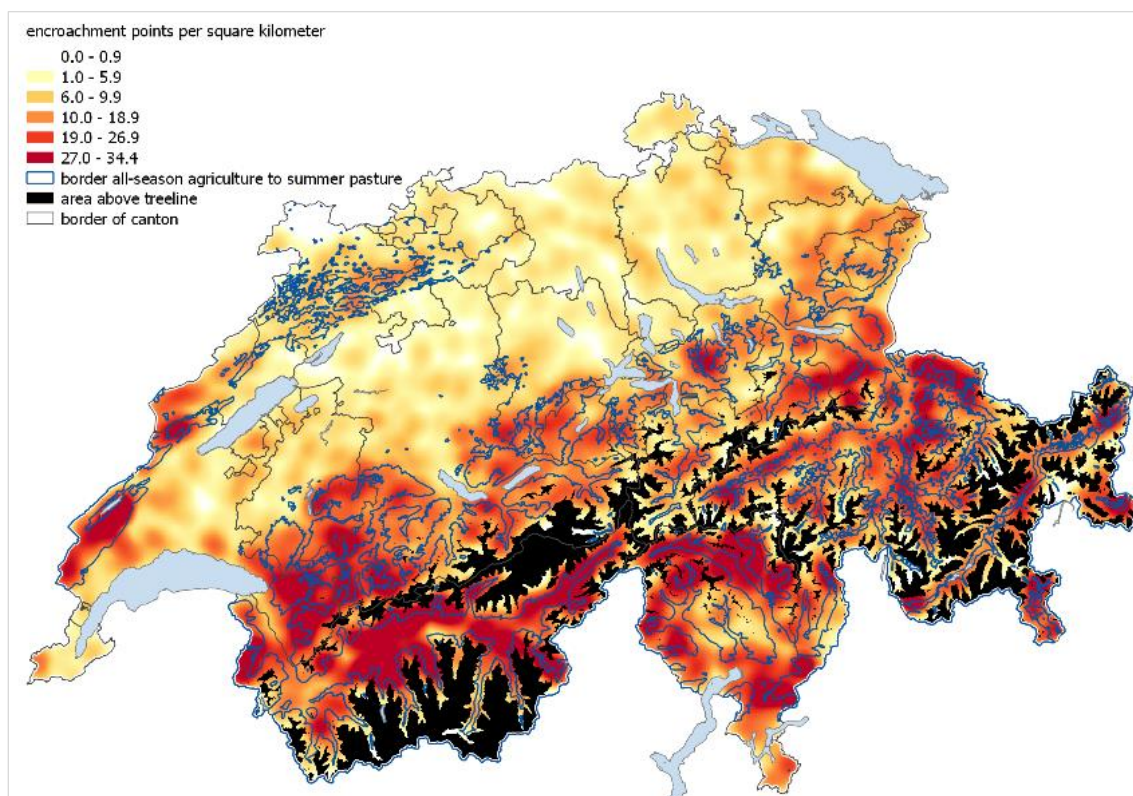
Figure 4: Belt of potential encroachment concentration (illustration by author, data: swisstopo[4], BLW.[5])

Overall, 2330 encroachment points remain (from a total of 10535 points) within an area of 500 m around the border from all-season agriculture to summer pastures (buffer

---

[4] Swiss Federal Office of Topography: swissTLM3D, swissalti3D
[5] BLW: Boundaries of agricultural zones

radius of 250 m). The encroachment belt covers an area of 10.6 % of the total area of Switzerland and 22.1 % of encroachment points.

Table 2: Encroachment points in potential encroachment belt, national

Canton	area [km²]	Total encroachment points	percentage of total area [%]	percentage of total points [%]	Points per km² in belt
Switzerland	41290.76	10535	100	100	0.251
belt area	4388.90	2330	10.6	22.1	0.531

Table 3: Encroachment points per canton with more than 0.40 p/km²

Canton	Total area [km²]	Total encroachment points	belt area [km²]	belt area percentage of total area [%]	points in belt	belt area percentage of total points [%]	Points per km² in belt
VS	5224.49	1957	496.6	9.5	368	18.8	0.74
TI	2812.21	1358	342.6	12.2	253	18.6	0.74
GR	7105.39	2157	1262.3	17.8	841	39.0	0.67
VD	3211.94	1049	243.6	7.6	126	12.0	0.52
BE	5959.59	1255	732.2	12.3	334	26.6	0.46
SZ	907.89	221	163.8	18.0	71	32.1	0.43
OW	490.58	165	63.8	13.0	27	16.4	0.42
NW	275.84	64	51.8	18.8	21	32.8	0.41
LU	1493.51	199	117.1	7.8	47	23.6	0.40

Table 36 (Appendix A) shows that wall-to-wall LiDAR data later than 2011 is only available for the cantons of Vaud and Berne. Due to the availability of data from the cadastral survey, the data of Berne were considered for further analysis.

In the canton of Berne eleven communes show a density above 0.20 encroachment points per square kilometre, from which five belong to the biogeographic region of the Jura (1) and six to the region of the Northern Alps (3).

Table 4: **Communes** in canton Bern with more than 0.20 encroachment points per km^2

	Commune	No. FSO	Total area [km^2]	Points in belt	Biogeographic region	Points per km^2
1	Grandval	694	8.25	5	1	0.61
2	Saxeten	591	19.42	10	3	0.51
3	Sauge	449	13.46	4	1	0.30
4	Horrenbach-Buchen	932	20.40	6	3	0.29
5	Saanen	843	120.06	35	3	0.29
6	St. Stephan	793	60.89	17	3	0.28
7	Lenk	792	123.09	32	3	0.26
8	Courtelary	434	22.21	5	1	0.23
9	Valbirse	717	18.68	4	1	0.21
10	Gsteig	841	62.43	13	3	0.21
11	Tramelan	446	24.83	5	1	0.20

2.5 Assessing of Shrub and Tree Encroachment

Observation of encroachment process can be easily done in the field over small areas, but monitoring large areas with remote sensing is challenging. Changes in land cover concern often small patches and discrimination from other land uses is difficult (Kolecka et al., 2015).

In forestry, many studies describe metrics for measuring 3D structure of forest, forest inventory, stem volume or biomass using LiDAR (Penner et al., 2015, Hyyppä et al., 2009, Blaschke, 2010). Using image-based point clouds, Wang et al. (2015) assessed short-term forest cover changes with good results for managed mixed forests. Van Ewijk et al. (2011) discriminated by assessing LiDAR based indices four stages of forest succession but not the stage of reforestation. Using multispectral images manly for forest change detection by Object Bases Image Analysis OBIA in combination with ALS data is widely used an achieves good results (Szostak et al., 2014, Blaschke, 2010). Waser et al. (2008) used CIR aerial images to asses change detection of forest and wooded area in mire biotope. Sahara et al. (2015) used repeat aerial photographic analysis and dendroecology for quantifying tree encroachment into a savannah.

Focusing on shrub and tree encroachment in grazing areas for livestock, literature and studies are rare. Anadón et al. (2014) recorded: "The impact of this global phenomenon [woody-plant encroachment] on livestock production, the main ecosystem service provided by grasslands, remains largely unexplored ".

3 Study Areas

Three study areas in Switzerland were chosen based on the following criteria:

1. Availability of ALS data
2. Different biogeographic region
3. High density of encroachment points (change of land use classification from agriculture to wooded area)

For the third criteria, data from the Swiss Land Use Statistics were analysed and integrated in chapter 2.4 Landscape Dynamic in Agriculture.

3.1 Available ALS Data

The countrywide ALS data set for Switzerland from the Federal Office of Topography swisstopo based on data collected between 2000 and 2007, providing a mean point density 0.5 points per square metre (Bundesamt für Landestopographie swisstopo, 2010a).

Furthermore, several cantons undertook their own flight missions for ALS data collection (compare flight year in Table 36, Appendix A). Fifteen cantons undertook their own flight mission between 2006 and 2015. Additionally, WSL collected ALS data for four larger areas in the canton Grison.

The raster in Figure 5 representing all available ALS data in Switzerland by point density.
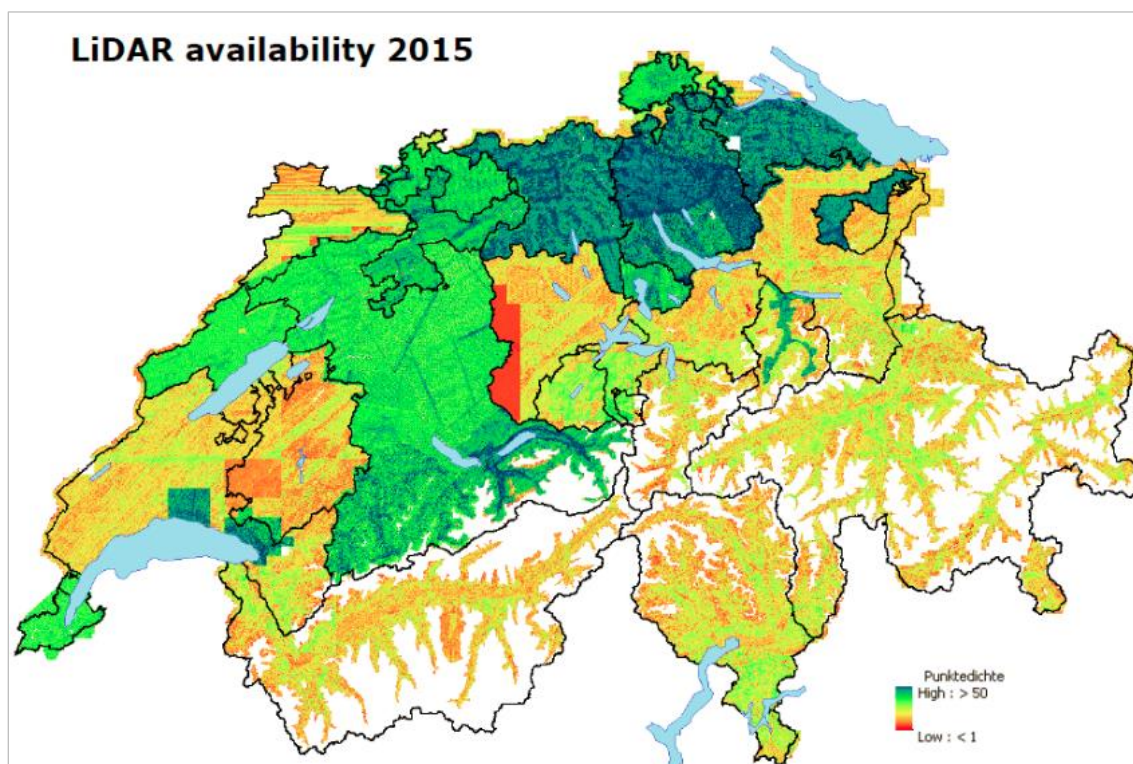
Figure 5: ALS data availability for Switzerland in 2015 illustrated by point density (Ginzler, 2016)

3.2 Biogeographic Regions

The biogeographical classification is based on patterns of the distribution of flora and fauna and consists of the six regions: Jura (1), Plateau (2), Northern Alps (3), Western Central-Alps (4), Eastern Central-Alps (5) and Southern Alps (6). The classification enables a better comparability of (biological) studies and serves as basis for current and future nature protection projects (Gonseth et al., 2001).

Figure 6: Biogeographic regions (illustration by author, data: swisstopo[6], BAFU[7])

---

[6] Swiss Federal Office of Topography: swissTLM3D

[7] BAFU: Bio-geographical regions

3.3 Study Areas Saxeten and Grandval

The selection of representative study areas was based on the availability of ALS data and different biogeographic regions in the same canton (Figure 7). The two communes Saxeten and Grandval with highest number of encroachment points per km^2, met the requirements. Due to unique conditions in the region of Maienfeld (canton Grison), an additional study area as described in chapter 3.4 was selected.
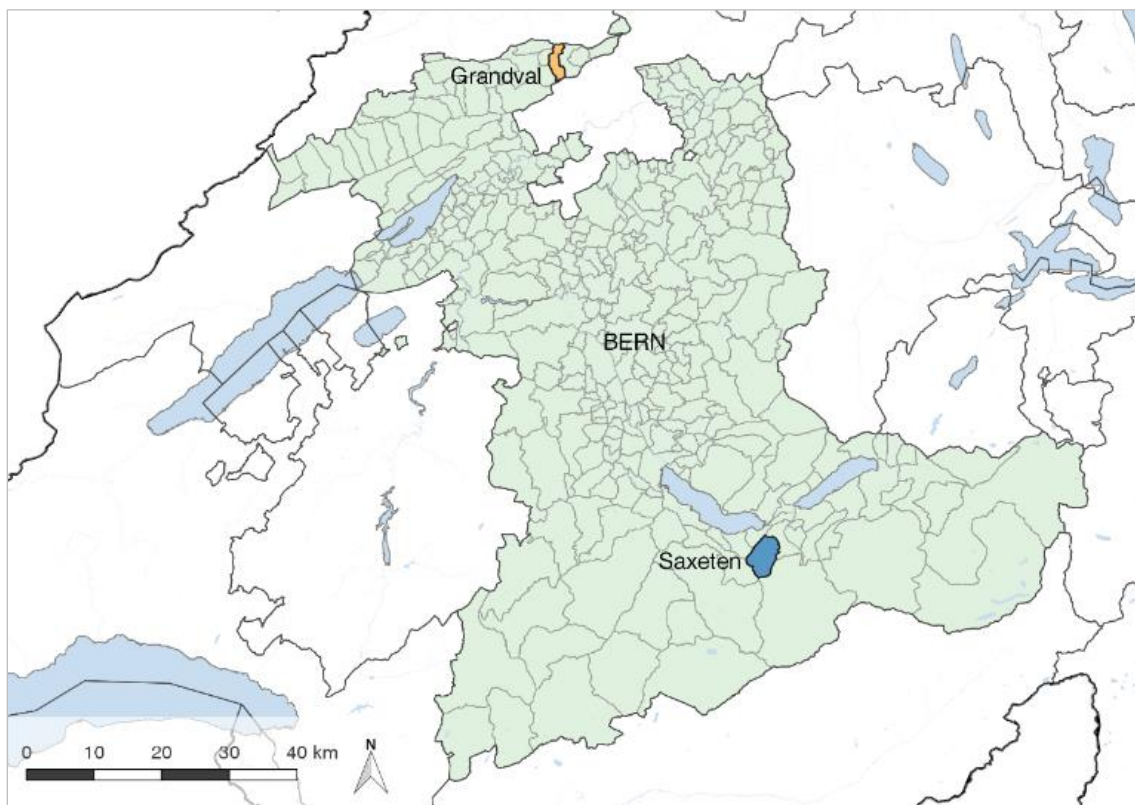
Figure 7: Overview canton Bern, study areas Grandval and Saxeten (illustration by author, data swisstopo[8], AGI[9])

Table 5 gives an overview of the land cover characteristics in the communes Saxeten and Grandval. Compared to the canton of Bern, areas of forest and agriculture of both Saxeten and Grandval are above average.

---

[8] Swiss Federal Office of Topography: swissTLM3D

[9] Amtliche Vermessung vereinfacht © Amt für Geoinformation des Kantons Bern

Table 5: Land cover area Saxeten and Grandval[10]

Study area	Total area	Forested area	Agriculture area	other	Elevation (m a.s.l.)
Saxeten	19.4 km^2	6.4 km^2	9.2 km^2	3.8 km^2	min: 820
	100 %	33.1 %	47.5 %	19.4 %	max:2724
Grandval	8.3 km^2	3.6 km^2	4.2 km^2	0.5 km^2	min: 565
	100 %	43 %	50.8 %	6.2 %	max: 1302
Canton BERN	5959.6 km^2	1701 km^2	2634.5 km^2	1624 km^2	min: 401
	100 %	28.5 %	44.2 %	27.3 %	max: 4274

Figure 8 gives an overview of land cover of the commune Saxeten and Figure 11 of the commune Grandval.
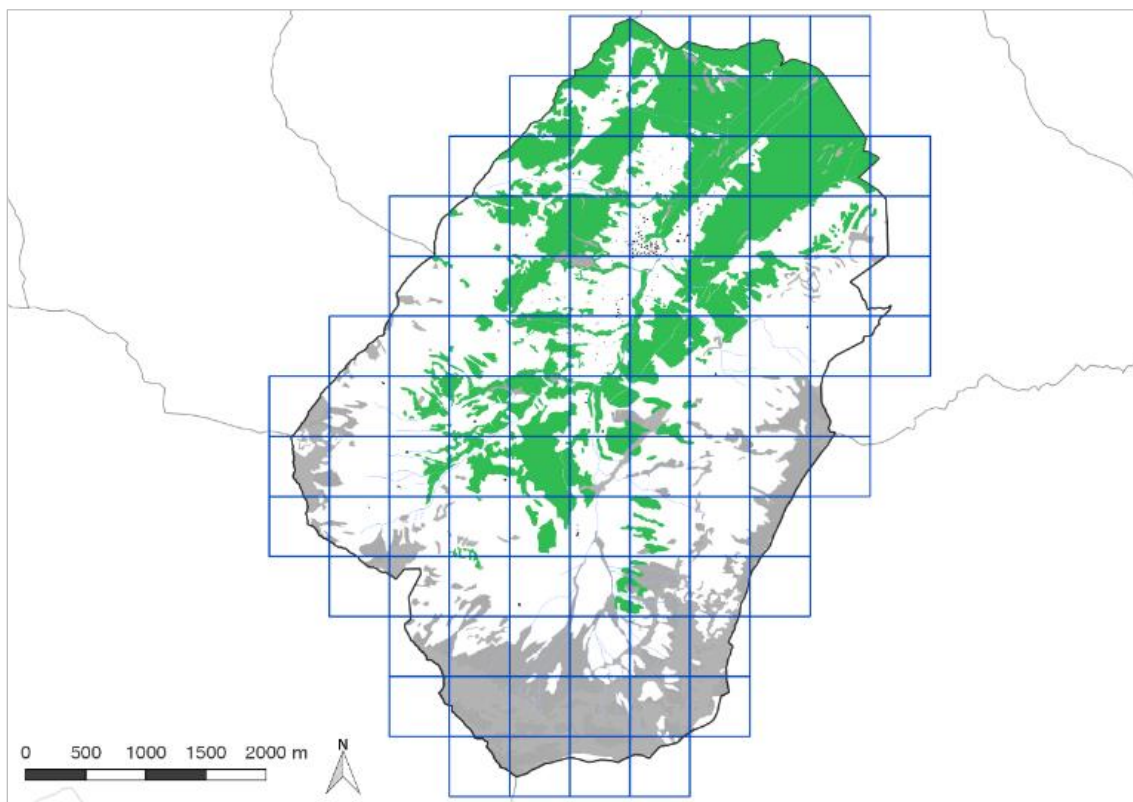
Figure 8: Commune Saxeten in the alpine region of the canton Bern (illustration by author, data: swisstopo[11], AGI[12]), green= forest, grey= rock, sand / white = agriculture area

---

[10] Data from cadastral survey of canton Bern (Amtliche Vermessung vereinfacht © Amt für Geoinformation des Kantons Bern / published: 15.09.2016). Minor variation to data from the Federal Office of Statistics due to generalisation of dataset.

[11] Swiss Federal Office of Topography: swissBoudaries3d

[12] Amtliche Vermessung vereinfacht © Amt für Geoinformation des Kantons Bern

Figure 9: Example of an area with typical shrub and tree encroachment in the pasture. (location: Sytiweideni, Saxeten, image by author, 26.09.2017)

Figure 10: The corresponding orthophoto from 2012
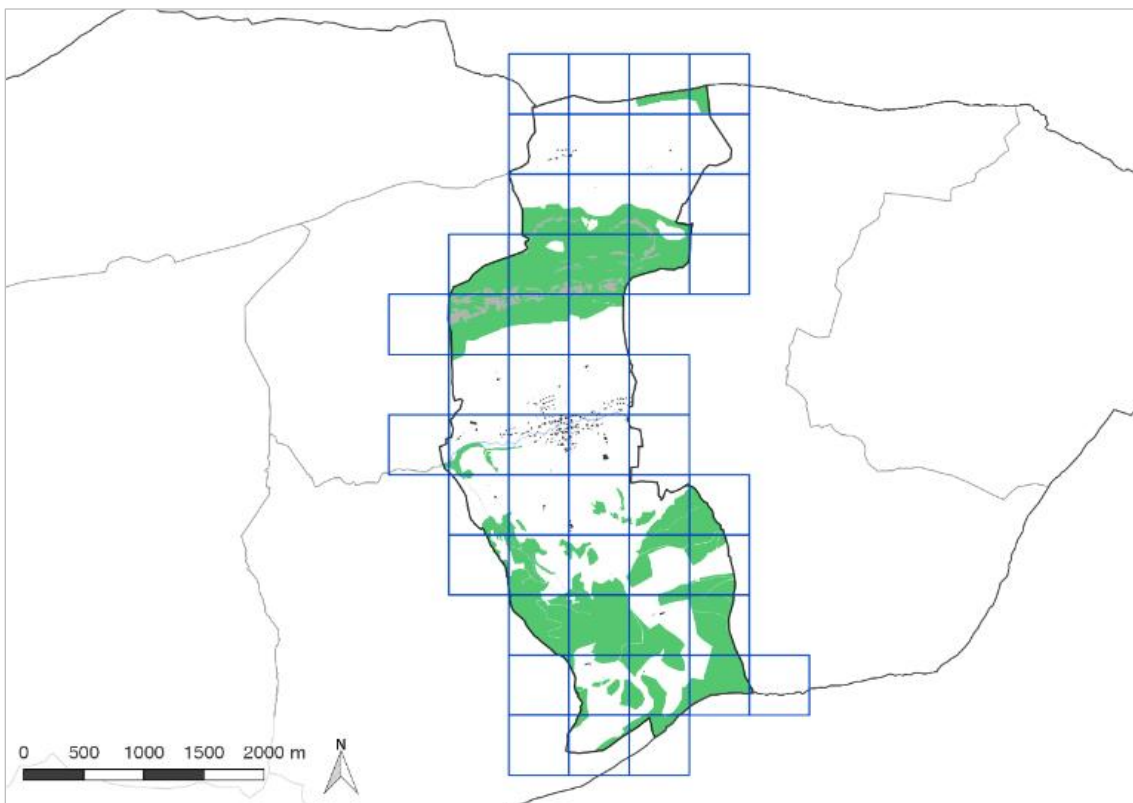
Figure 11: Commune Grandval in the Jura region of canton Bern (illustration by author, data: swisstopo[13], AGI[14]), green= forest, grey= rock, sand / white = agriculture area

---

[13] Swiss Federal Office of Topography: swissBoudaries3d

[14] Amtliche Vermessung vereinfacht © Amt für Geoinformation des Kantons Bern

3.4 Study Area Maienfeld

The area around the commune of Maienfeld in the canton Grison characterized by a relatively high ALS point density in the acquisition from 2002. During the investigations in the framework of this thesis, the area of Maienfeld stood out with its point density of more than 4 points per square meter. Moreover, WSL collected data from the same area in 2015 with a very high point density of more than 20 points per square meter. The extension of the area is exactly one tile (13.14 km^2) of the orthophoto mosaic Swissimage from swisstopo. These data were probably collected for testing purposes.
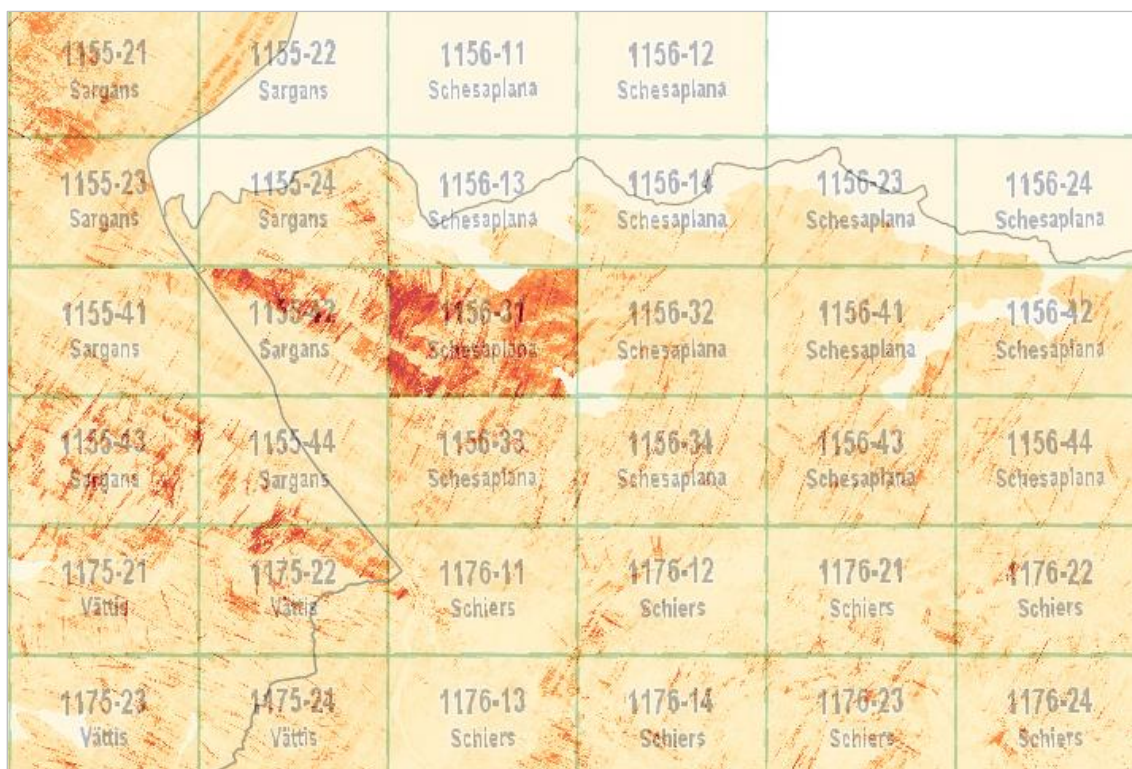
Figure 12: Area 1156-31, near Maienfeld in canton Grison, point density of data collected in 2002 (illustration by author, data: swisstopo[15], WSL[16])

[15] Swiss Federal Office of Topography: swissBoudaries3d
[16] Normalised LiDAR data 2015, WSL
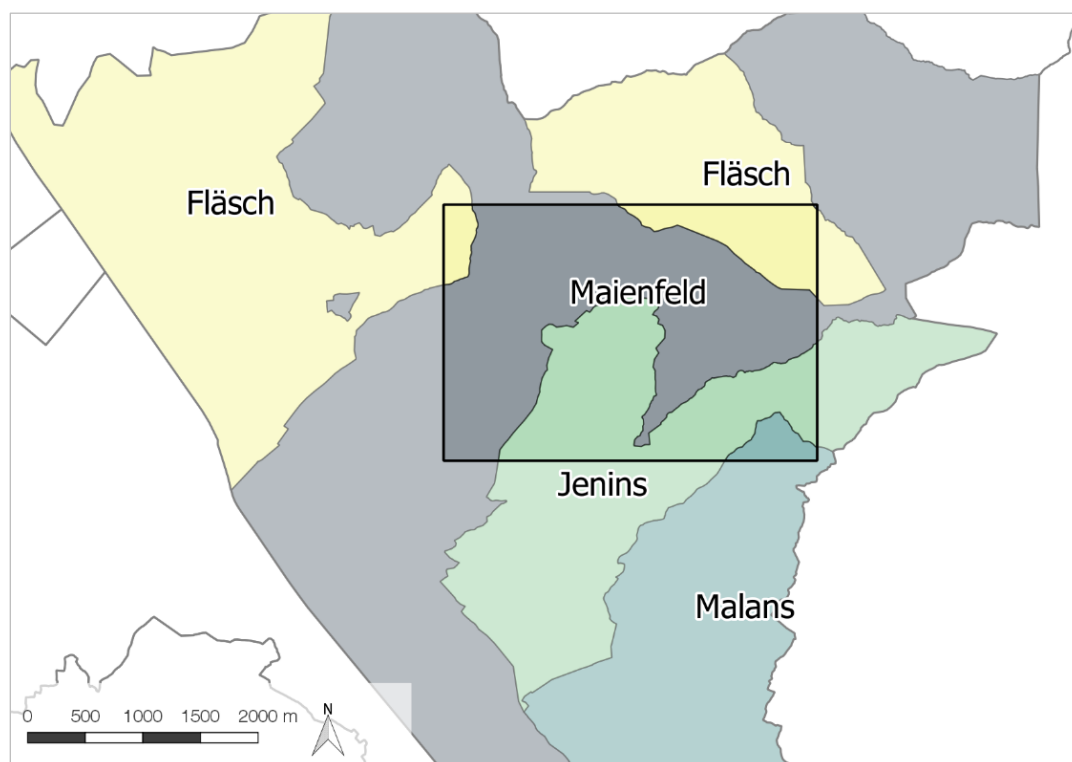
Figure 13 Communes Maienfeld, Malans, Fläsch and Jenins in canton Grison (illustration by author, data: swisstopo[17])

The area covers parts of the communes Maienfeld, Malans, Fläsch and Jenins. The values

for land cover categories has been calculated based on the cadastral survey.

Table 6: Land cover area Maienfeld[18]

Study area	Total area	Forested area (%)	Agriculture area	other	Altitude (m a.s.l.)
Maienfeld [area 1156-31]	13.14 km²	6.69 km²	5.36 km²	0.83 km²	min: 606
	100 %	52.9 %	40.8 %	6.3 %	max:2445

---

[17] Swiss Federal Office of Topography: swissBoudaries3d

[18] Cadastral survey, source: Amtliche Vermessung (AV), Kanton Graubünden, 17.09.2017
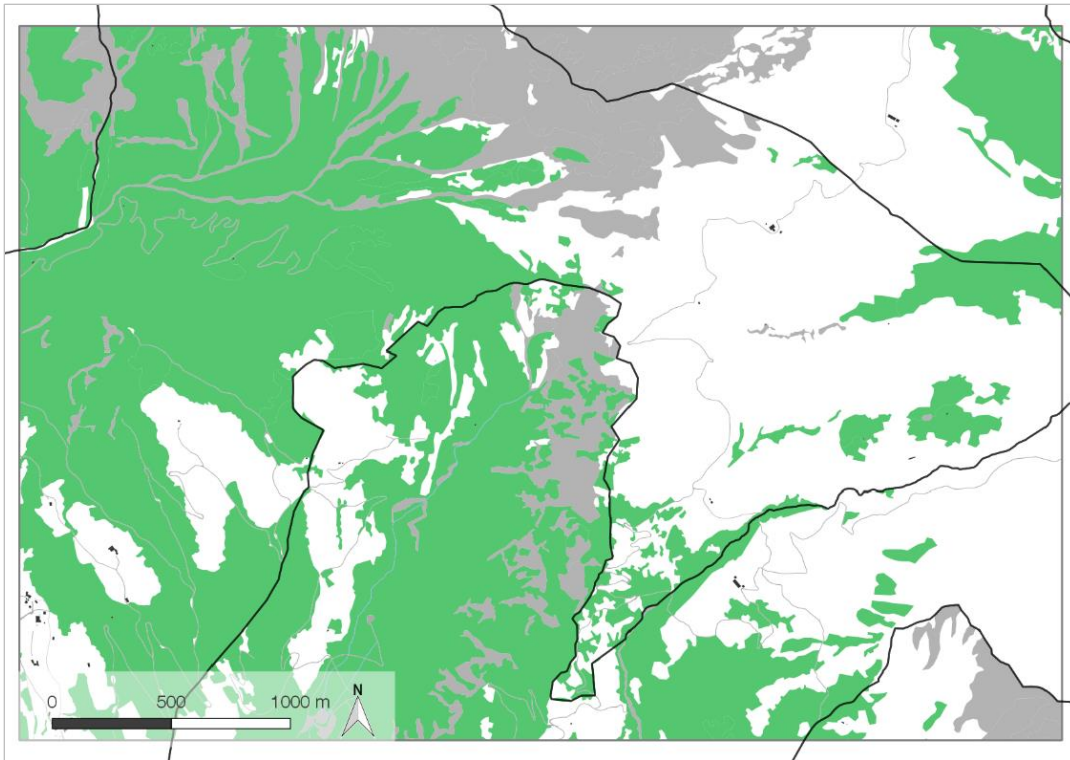
Figure 14 Communes Maienfeld, Malans, Fläsch and Jenins in canton Grison (illustration by author, data: swisstopo[19], Kanton Graubünden[20]) green= forest, grey= rock, sand / white = agriculture area

The area is characterized by forest from the lower to the middle part up to the treeline around 1700 to 1800 m a.s.l. Above the treeline, land is mainly used as alpine pastures and meadows. This area between the summit Vilan (2375 m) and Glegghorn (2445 m) is characterized by fens and shrub vegetation.

---

[19] Swiss Federal Office of Topography: swissBoudaries3d, tilling Swissimage

[20] Cadastral survey, source: Amtliche Vermessung (AV), Kanton Graubünden, 17.09.2017

4 Materials and Methods

In order to identify shrub and tree encroachment, two data sets from different years are required. The optimal time interval depends on the aim of the data comparison and the accuracy of the collected data. In this thesis, the focus was laid on shrub and tree vegetation located between 600 and 2200 m a.s.l. in Switzerland.

Growth of trees and shrubs depends on several parameter such as exposition, altitude, soil, precipitation etc. For example, the impact of altitude to the height growth of spruce (Picea abies) has been examined by Holzer (1967) who observed an annual height growth of 22cm in areas around 1400 m a.s.l.

The accuracy of the used ALS data from 2001 and 2002 is around ±50cm for height (Bundesamt für Landestopographie swisstopo, 2010a). The data collected by the canton of Berne in 2012 have an height accuracy of less than ±20cm (Amt für Wald des Kantons Bern, 2014). In order to detect new grown spruces with a height of 50cm using these data, a minimum time difference of five to eight years is required.

Old ALS data and the ALS data of Berne were collected under leave-off conditions between the end of autumn and start of spring. To minimize the influence of grass vegetation on pastures, this is a decisive point for encroachment identification. ALS data in the area of Maienfeld was collected in August 2015, under leave-on conditions. These specific conditions are essential for the interpretation of the results.
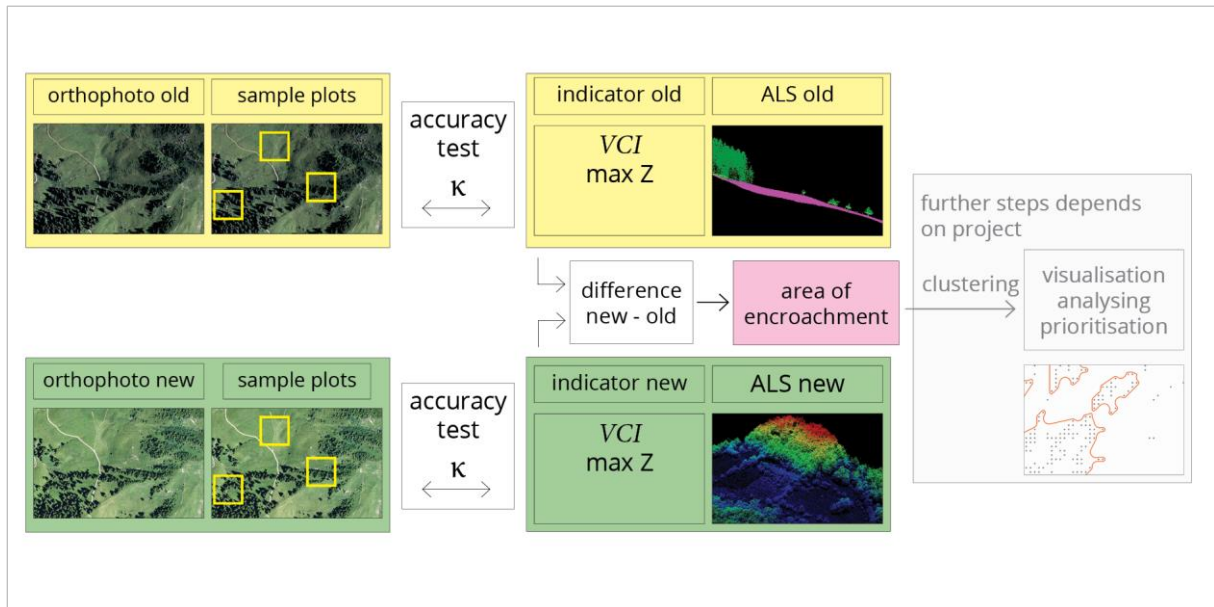
Figure 15 Concept and workflow of data analysis

Figure 15 shows the workflow of analysing the old and new orthophotos and the ALS data, which is carried out for every study area. The accuracy of the calculated Vertical Complexity Index (VCI, see chapter 4.2) combined with a maximum Z value is proofed compared to manually digitized information. For each orthophoto, 450 sample plots were classified. The area of shrub and tree encroachment is obtained from the difference between the calculated indicator from old and new ALS data. In the following chapters input data, the VCI, software and the workflow will be described.

4.1 Data

ALS Data I

The first ALS data set was acquired by swisstopo between 2000 and 2007. The data was first normalised and then merged into tiles of 5 by 5 km by WSL for other ALS based studies. The used ALS data have the following characteristics for the three study areas of this thesis: Density in Table 7 and Table 8 was calculated for LAZ-tiles clipped with the corresponding boundary of study area using lasinfo from Lastools (Isenburg, 2017).

Table 7: ALS data I

Study area	flight year	density [p/m^2]	Size of tile [km^2]	Tiles cover study area	Tiles name
Saxeten	October 2001	1.5	25	4	nDSM_625000_165000.laz nDSM_630000_165000.laz nDSM_625000_160000.laz nDSM_630000_160000.laz
Grandval	October 2001	1.2	25	4	nDSM_595000_235000.laz nDSM_600000_235000.laz nDSM_595000_230000.laz nDSM_600000_230000.laz
Maienfeld	March 2002	4.2	25	2	nDSM_760000_205000.laz nDSM_760000_210000.laz

ALS Data II

The second ALS data set for Saxeten was acquired by the canton of Bern in April 2012 and for Grandval in April 2011. For all analyses the raw point cloud data were used (Amt für Wald des Kantons Bern, 2014).

For the study area Maienfeld, a dataset with a high point density of more than 20 points/m^2 was used, which was acquired by the WSL in August 2015.

Table 8: ALS data II

Study area	flight year	density [p/m^2]	Size of tile [km^2]	Tiles cover study area	Tiles name
Saxeten	April 2012	18.9	1	30	627_162.laz, 627_163.laz, 627_164.laz, 628_160.laz, 628_161.laz, 628_162.laz, 628_163.laz, 628_164.laz, 628_165.laz, 629_160.laz, 629_161.laz, 629_162.laz, 629_163.laz, 629_164.laz, 629_165.laz, 629_166.laz, 630_160.laz, 630_161.laz, 630_162.laz, 630_163.laz, 630_164.laz, 630_165.laz, 630_166.laz, 631_162.laz, 631_163.laz, 631_164.laz, 631_165.laz, 631_166.laz, 632_164.laz, 632_165.laz
Grandval	April 2011	9.8	1	19	597_236.laz, 597_237.laz, 598_234.laz, 598_235.laz, 598_236.laz, 598_237.laz, 598_238.laz, 598_239.laz, 599_234.laz, 599_235.laz, 599_236.laz, 599_237.laz, 599_238.laz, 599_239.laz, 600_234.laz, 600_235.laz, 600_236.laz, 600_238.laz, 600_239.laz
Maienfeld	August 2015	21.7	1	18	764000_211000.laz, 764000_210000.laz, 764000_209000.laz, 763000_211000.laz, 763000_210000.laz, 763000_209000.laz, 762000_211000.laz, 762000_210000.laz, 762000_209000.laz, 761000_211000.laz, 761000_210000.laz, 761000_209000.laz, 760000_211000.laz, 760000_210000.laz, 760000_209000.laz

Orthophotos

The Federal Office of Topography swisstopo provides geometrically corrected aerial photographs (orthophotos). For the study area Saxeten, the orthophotos available date from 2004 and 2012. For the study area Grandval, orthophotos from 2004 and 2011 are available. From the year 2001, when ALS data was collected no orthophotos are available. The ground pixel size of the orthophotos before 2005 is 0.5 m and after 2005 0.25 m for areas below 2000 m a.s.l. (Bundesamt für Landestopographie swisstopo, 2010b / Bundesamt für Landestopographie swisstopo, 2008).

For study area Maienfeld the orthophotos available date from 2002 and 2014 corresponding with the ALS data collection years of 2001 and with one year difference to the second ALS data set from 2015.

Table 9: Orthophotos study area

Study area	Year	Ground pixel size [m]	Tiles cover study area	Tiles name
Saxeten	2004 2012	0.5 0.25 / 0.5	4	1228-14 / 1228-23 / 1228-32 / 1228-41
Grandval	2004 2012	0.5 0.25	4	1106-22 /1106-23 / 1106-24 / 1106-42
Maienfeld	2002 2014	0.5 0.25	1	1156-31

4.2 Vertical Complexity Index VCI

The Vertical Complexity Index is an implementation of the concept of evenness to a LiDAR point cloud for quantifying the vertical distribution of the points. It is based on the information theory index developed by Shannon (1948), which has been used to quantify species diversity and species evenness in ecology. The evenness index should be at a maximum, when in a sample all species are equally abundant and should decrease towards zero, as the relative abundances of species become more and more unequal (van Ewijk et al., 2011, Penner et al., 2015).

$$VCI = (-\sum_{i=1}^{HB}[(p_i) \cdot \ln(p_i)])/\ln(HB)$$

A normalised point cloud is divided into a number of height bins HB. The number of LiDAR returns per height bin as a proportion of the total number of LiDAR returns is used to define p_i.

A VCI value close to 1 indicates that most height bins have equal numbers of points. As the distribution of points per height bin becomes more uneven, VCI decreases (van Ewijk et al., 2011).
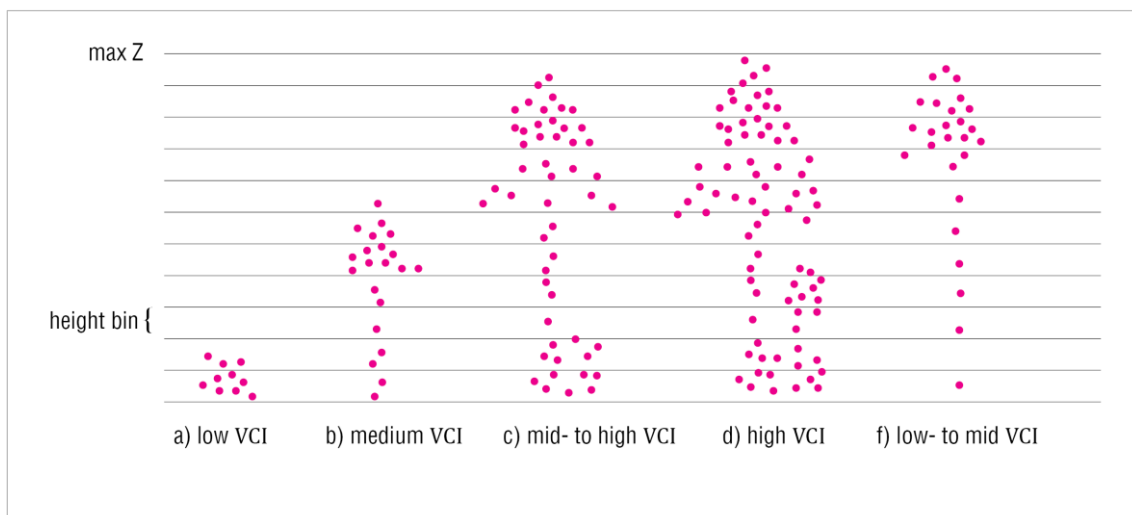
Figure 16: Expected value of Vertical Complexity Index VCI (illustration by author, values: van Ewijk et al., 2011)

Figure 16 shows the expected VCI value for different stages (a-d) of the vegetation development: a) low VCI values for small vegetation such as shrub and tree encroachment, when all returns are concentrated in the lowest height bin(s); b) mid-range VCI values for the stem exclusion stage, as returns are concentrated in a grouping of

height bins representing the upper canopy; c) for the understory re-initiation stage mid-to high VCI values are expected, as returns would be concentrated in two separate groupings of height bins. Finally, (d) for an old growth stage a high VCI value, since returns are expected to be more evenly distributed over the entire vertical column (van Ewijk et al., 2011).

The authors investigated the differentiation between stages of forest succession, but not the differentiation between pastures (no forest) and initiation stage. For stem exclusion stage, same authors measured a mean VCI of 0.63, for the understory re-initiation stage 0.75, and for old growth stage 0.80.

4.3 Software

Point Data Abstraction Library PDAL

PDAL is an open source software (BSD-licence) for basic point cloud processing operations like translation, filtering, clipping and exploitation. It allows to compose operations on point clouds into pipelines of stages (Butler and Gerlek, 2017). To run the pre-built version of PDAL on Windows the containerization software Docker is used.

Used Version: 1.5

RStudio

RStudio is an integrated development environment (IDE) for R and is licenced under GNU as open source[21] software (R Development Core Team, 2017). It was preliminary used in this thesis for executing the calculation of the VCI (see 4.2, page 45), which is provided by the package lidR (Roussel, 2017). The functions provided by package rLiDAR (Silva et al., 2015) have been tested for the calculation of the Canopy Height Model (CHM) and the LiDAR-processing of small sample data set, but not for the final processing. The well working functions of the package rLIDAR did not fit the requirements of shrub and tree detection in alpine pastures.

Used Version: 1.0.136

LasTools

LasTools is a powerful tool package for processing LiDAR data. It provides scriptable tools with multi-core batching. In this thesis only the free to use parts of the tools were tested (see chapter 2.2) and finally las2las and lasinfo (-compute_density) was used for pre-processing and point density calculation (Isenburg, 2017).

Used Version: 170628

---

[21] https://cran.r-project.org/doc/FAQ/R-FAQ.html

QGIS

QGIS was used in this thesis for exploring intermediate results, analysing and processing vector and raster data, and for the visualisation of the final results (QGIS Development Team, 2017).
Used Version: 2.14.19-Essen

PostgreSQL/PostGIS

PostgreSQL is an open source object-relational database management system. PostGIS is a spatial database extender for PostgreSQL and adds support for geographic objects allowing location queries to be run in SQL (PostgreSQL Global Development Group, 2017/ Refractions Research et al., 2017). The database was used to store results from R-processing and PostGIS for calculating the combined indicator of VCI and maximum Z value and for excluding areas based on land use classification from the cadastral survey.
Used Version: PostgreSQL 9.5.7 / PostGIS 2.2.1

4.4 Calculation of Shrub and Tree Encroachment Indicator

For both ALS datasets, an encroachment indicator was calculated as shown in Figure 17. In a first step, DTMs were generated based on the ALS data. Then both altitude and slope data from the DTM were used to exclude all areas that are of no agricultural interest (compare chapter 2.3). Secondly, ground and vegetation points were filtered and normalised and the VCI was calculated (see chapter 4.2). Thirdly, maximum Z value, a further criteria for exclusion of established trees from the final encroachment indicator was generated from normalised vegetation data.
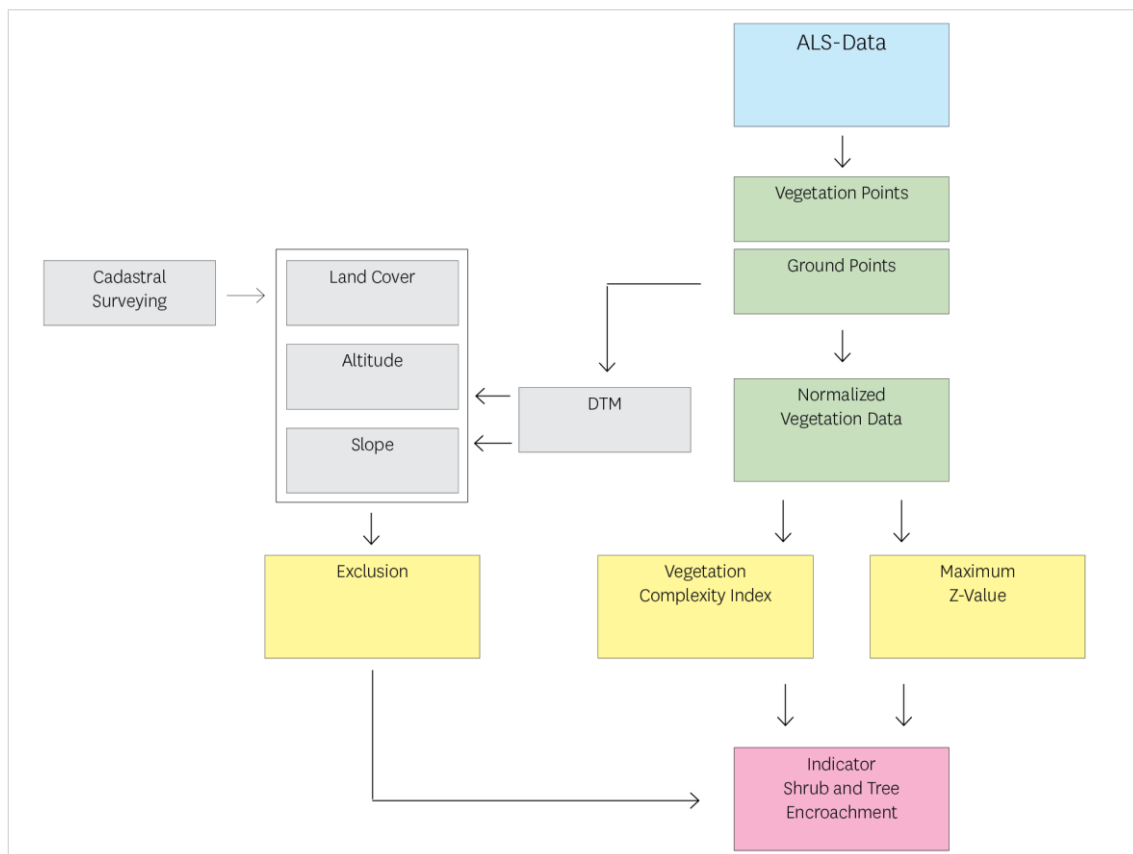
Figure 17: Process indicator calculation

Grid Cell Size

In order to implement the tested approach for large areas, particular attention during testing was paid on scalability and computation costs. Van Ewijk et al. (2011) used circular plots with an area of 400 m^2 (radius = 11.28 m). The used implementation in R-package

lidR required a squared plot cell. Testing different cell size revealed a grid cell size of 3 m is a suitable compromise between accuracy and computation costs (see chapter 4.5).

Pre-processing

ALS data were normalised with PDAL. In order to process all files of a folder, a pipeline (code in Table 10) executes the filter 'Height Above Ground' (*filters.hag*[22]). In a first step, the filter calculates the height above the nearest (x,y) ground point for each point in the point cloud according the ASPRS classes for vegetation 3, 4 and 5 (ASPRS, 2013).

In a second step, points with Z values bellow zero and above 50 m are dropped with *filters.range*[23] and only points classified as vegetation are selected and written to a new LAZ file.

Table 10: Code pipeline for Docker, vegetation normalization

```
{
 "pipeline":[
  "/data/629_165.laz",
  {
   "type":"filters.hag"
  },
  {
   "type":"filters.ferry",
   "dimensions":"HeightAboveGround = Z"
  },
  {
   "type":"filters.range",
   "limits":"Z[0:50], Classification[3:5]"
  },
  {
   "type":"writers.las",
   "filename":"/data/629_165_v_norm50.laz"
  }
 ]
}
```

---

[22] https://www.pdal.io/stages/filters.hag.html (visited 19.05.2017)
[23] https://www.pdal.io/stages/filters.range.html (visited 19.05.2017)

For looping through all files in a folder, the pipeline in Table 12 is executed in Docker by code as described in Table 11. One problem of Docker for Windows is to keep the container running until the loop script has started. The 'tail –f /dev/null' command keeps the container running in the foreground, even when the main command runs in background[24].

Table 11: Run Docker on Windows and execute code from loop.sh

```
PS C:\> docker run -d -v /c/data:/data pdal/pdal:1.5 tail -f /dev/null
PS C:\> docker exec -it
    67f8d1f857a3ee6d41ba193f28ee0812b17a0a4d155e3a56c2b22af3542d4534
    /bin/bash
PS C:\> /data/loop/.loop.sh
```

Table 12: Code looping through all files

```
s *.laz | xargs –I{} pdal pipeline -i /data/pipeline_hag_norm.json --readers.las.filename=out/{} --writers.las.filename=hag/{}
```

Generating Digital Terrain Model

The DTM is generated with PDAL using the same workflow as described above, but with adapted pipeline (see Table 13).

Table 13: Code pipeline for Docker, DTM

```
{
 "pipeline":[
    "/data/631_176_2.laz",
    {
   "type":"filters.range",
   "limits":"Classification[2:2]"
  },
  {"type":"writers.gdal",
      "resolution": 1,
      "output_type": "mean",
      "output_format":"tif",
```

---

[24] https://stackoverflow.com/questions/30209776/ (visited 02.06.2017)

```
        "filename":"/data/631_176_mean.tif"
    }
  ]
}
```

VCI Calculation

VCI is calculated based on the normalised vegetation LAZ files with the package lidR in R.

Table 14: Code VCI calculation in R

```
lasFiles <- list.files(startingDir, pattern = ".laz", full.names = TRUE)
for (fileName in lasFiles) {
 las = readLAS(fileName)
 vci = las %>% grid_metrics(VCI(Z, by=1, zmax = 40), res = 3)
 vci2 <- data.table(vci)[, .(X, Y,V1)]
 names(vci2)[names(vci2)=="X"] <-"x"
 names(vci2)[names(vci2)=="Y"] <-"y"
 names(vci2)[names(vci2)=="V1"] <-"vci"
 dbWriteTable(con, c("master","be_vci12"), value=vci2, append=TRUE, row.names = FALSE)}
```

Maximum Z Value

Z elevation in a 3 m grid is calculated based on the normalised vegetation LAZ files with the package lidR in R.

Table 15: Z-max calculation in R for all tiles in folder

```
lasFiles <- list.files(startingDir, pattern = ".laz", full.names = TRUE)
for (fileName in lasFiles) {
 las = readLAS(fileName)
 zmax = las %>% grid_metrics(max(Z), 3)
 zmax2 <- data.table(zmax)[, .(X, Y,V1)]
 names(zmax2)[names(zmax2)=="X"] <-"x"
 names(zmax2)[names(zmax2)=="Y"] <-"y"
 names(zmax2)[names(zmax2)=="V1"] <-"zmax"
 dbWriteTable(con, c("master","be_zmax12"), value=zmax2, append=TRUE, row.names = FALSE)}
```

Combining VCI and Maximum Z Value

The Vertical Complexity Index can be low even if maximum height (Z) is higher than expected (compare Figure 16, page 45). Thus, the maximal Z value is cell-wise computed from the CHM and excluded if Z is below 0.2 m or above 3.6 m. With the lower limit, returns from short vegetation (e.g. grass) are excluded. According to the Swiss National Forest Inventory (LFI), 3 m is the minimal tree height of forest (Brassel, 2001). Values of VCI smaller than 0.01 and higher than 0.61 are also excluded (derivation of threshold see chapter 5.1).

Table 16: Classifying VCI and z-max

```
##encroachment indicator old data
DROP TABLE master.be_index02;
CREATE TABLE master.be_index02
AS SELECT vci,zmax, be_vci02.geom, be_vci02.gid
FROM master.be_vci02, master.be_zmax02 WHERE ST_Within(be_vci02.geom, be_zmax02.geom)
AND vci BETWEEN 0.01 AND 0.61 AND zmax BETWEEN 0.2 AND 3.6

##indicator new data
DROP TABLE master.be_index02;
CREATE TABLE master.be_index12
AS SELECT vci,zmax, be_vci12.geom, be_vci12.gid
FROM master.be_vci12, master.be_zmax12 WHERE ST_Within(be_vci12.geom, be_zmax12.geom)
AND vci BETWEEN 0.01 AND 0.61 AND zmax BETWEEN 0.2 AND 3.6
```

Difference between Old and New Indicator Values

Differences between new and old indicator values were calculated in PostGIS using the code shown in Table 17.

Table 17: Extract difference of VCI old and VCI new in PostGIS

```
##difference old to new
CREATE TABLE master.be_diff AS SELECT i12.gid, i12.vci, i12.zmax, i12.geom
FROM master.be_index12 as i12 LEFT JOIN
master.be_index02 as i02 ON
ST_WITHIN(i12.geom, i02.geom)
WHERE i02.gid IS NULL;
SELECT DISTINCT gid, count(gid) as count FROM master.be_diff GROUP BY gid ORDER BY count desc;
ALTER TABLE master.be_diff ADD PRIMARY KEY(gid);
```

4.5 Ground Truth and Sampling Design

Orthophoto Interpretation

The validation is based on a comparison calculated indicator from ALS data, classified as shrub and tree encroachment and the results of orthophoto interpretation.

Obviously, orthophotos interpretation using a 3 m grid led to operational difficulties due to the 0.5 m spatial resolution of the orthophotos from 2004 since 3 m are 36 pixels, 9 m 324 pixels and a 12 m are 576 pixels (see Figure 18, Figure 19).
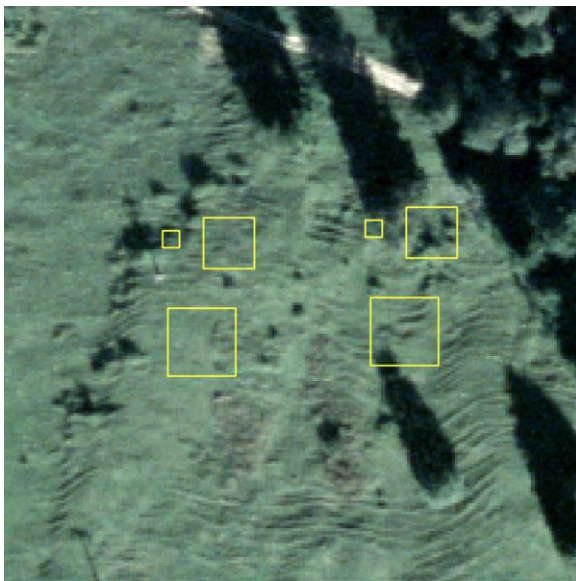
Figure 18: Evaluation cell size for orthophoto interpretation, side length 3, 9 and 12 m (orthophoto 2004, Grandval)

Figure 19: Evaluation cell size for orthophoto interpretation (orthophoto 2012, Grandval)

For this reason, regular grids of 3, 9 and 12 m were tested (see Figure 18 and Figure 19). Interpretation of smaller orthophoto samples is more difficult and leads to uncertainty of classification. The test revealed that a 12 m grid was most appropriate regarding accuracy and operational efficiency.

Sample Size

Based on the study of Foody (2009), which analyses sample size determination for image classification accuracy assessment, the following approach was adopted to determinate sample size.

For an initial estimate of the minimum required sample size the same author suggests:

$$n' = \left[\frac{z_\alpha\sqrt{P_0(1-P_0)} + z_\beta\sqrt{P_1(1-P_1)}}{P_1 - P_0}\right]^2$$

Where n' is the target sample size, P_0 Proportion (accuracy of orthophoto interpretation), P_1 accuracy of a classification (indicator derived form LiDAR data). Foody (2009) recommends to refine the sample size through the inclusion of a continuity correction.

$$n = \frac{n'}{4}\left(1 + \sqrt{1 + \frac{2}{n'|P_1 - P_0|}}\right)$$

Thus using P_0 = 0.85 and P_1= 0.90, z_α = 1.95, z_β=0.8 the results in n' = 350.7 and n = 370.4, respectively. Based on a confidence interval of 95% and sampling errors of 5% 370 sample plots remain. Additional 20% were added for supposedly unclassified samples, 450 cells were randomly selected outside of the exclusion layer.
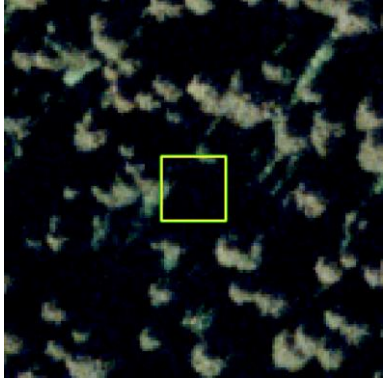
Table 18: Random sample in R

```
## aggregation of exclusion layer to cells of 12 m
excl1 <-aggregate(excl, fact=4, fun=max)
excl2 <- mask(excl1, gmd_sax) ## or gmd_gdv or area_mf

sp12 <- sampleRandom(excl2, size=450, asRaster=TRUE)
pol <- rasterToPolygons(sp12, fun=NULL, n=4, na.rm=TRUE, digits=12, dissolve=FALSE)
## Write sample cells to PostgreSQL DB
dbWriteTable(con, c("master","sample450"), value=pol, append=TRUE, row.names = FALSE)}
```

The 450 plots per study area have been evaluated and categorized as sample plots with shrub and tree encroachment and plots without. The threshold for the class *shrub and tree* is set in the case of at least ¼ of the area is covered. Forested areas or areas with large trees were assigned to *unclassified*. Plots that are affected by shadow of e.g. large trees or the topography were assigned to *unclassified* as well (see Table 19 on next page).

Table 19: Examples of orthophoto classification

	2004	2012
2004: no shrubs and trees 2012: no shrubs and trees	 103_04	 103_12
2004: shrubs and trees 2012: shrubs and trees	 71_04	 71_12
2004: other (less than ~1/4 of the area is covered by shrubs and trees) 2012: unclassified due to shadows	 374_04	 374_12
2004: unclassified due to shadows 2012: shrubs and trees	 7_04	 374_12

4.6   Aggregation of the Encroachment Indicator

To compare the encroachment indicator, calculated in a 3 m grid, with the results from orthophoto interpretation (grid size 12 m), an aggregation was executed.

The final shrub and tree encroachment indicator saved as raster provides the information of encroachment per grid cell as value 0 for no encroachment and as value 1 for cells classified as shrub and tree encroachment. With executing cell statistics, this information is summarised for each sample plot. When all 3 m grid cell in a sample plot are classified as *shrub and tree*, a value of 16 is written to the given sample plot. When four or more cells from the grid are classified as *shrub and tree* the sample plot is interpreted as encroachment plot. This threshold is based upon the threshold for orthophoto interpretation (see chapter 4.5).

The sample plot on the right side in Figure 20 (blue square) contains five cells from the encroachment indicator classified as *shrub and tree*, is aggregated to a sample plot with encroachment. The left square contains only two cells classified as *shrub and tree* and is therefore interpreted as sample plot without encroachment.
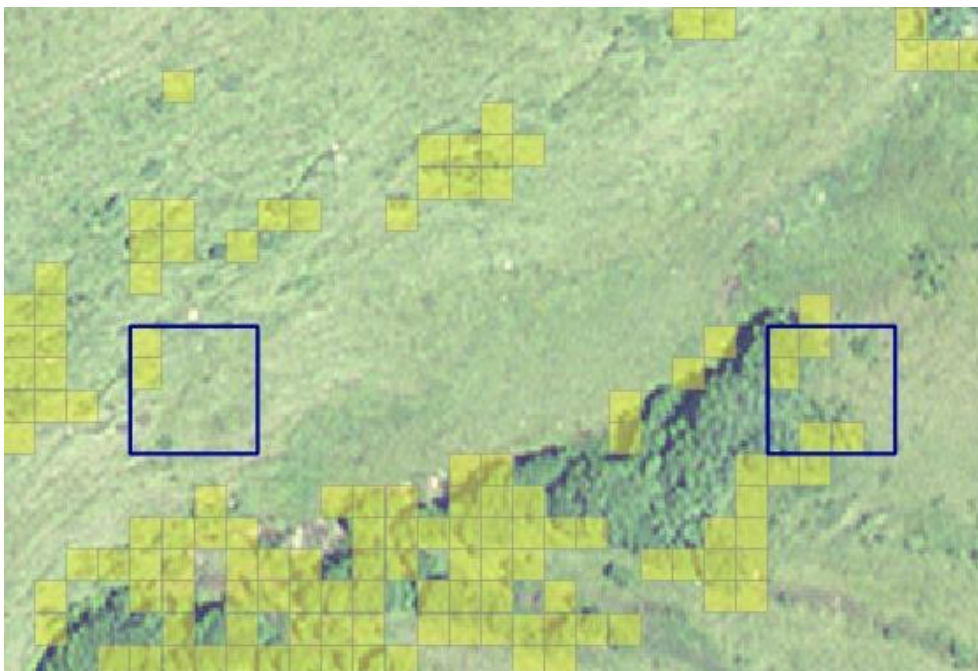
Figure 20: Aggregation of 3m grid information to 12 m sample plot

4.7 Accuracy Assessment

Data from orthophoto interpretation were used as reference data for the accuracy assessment. The number of correctly classified sample plots by the encroachment indicator calculation are A and D in Table 20. Hence, the producer's accuracy for class *shrub and tree* is from primary interest.

Table 20: Accuracy assessment of encroachment indicator and Kappa calculation

| | | classified (ALS data) | | | |
		other (plots)	shrub and tree (plots)	Totals (plots)	User accuracy (%)
reference (orthophoto)	other (plots)	A	B	$A+B$	$\dfrac{A}{A+B}$
	shrub and tree (plots)	C	D	$C+D$	$\dfrac{C}{C+D}$
		$A+C$	$B+D$	$A+B+C+D$	
Producer's accuracy (%)		$\dfrac{A}{A+C}$	$\dfrac{B}{B+D}$		
Kappa coefficient :	$\dfrac{overall\ accuracy - random\ result}{1 - random\ result}$				
Random result:	$\dfrac{(A+C)*(A+B)+(B+D)*(C+D)}{(A+B+C+D)^2}$				

The Kappa coefficient, introduced by Cohen (1960), is widely used in accuracy assessment of remotely sensed data (Hofmann, 2015, Schaepman et al., 2015). Although newer discussions suggest using other indices than Kappa for accuracy assessment in remote sensing (Pontius Jr and Millones, 2011), the Kappa coefficient is used for this thesis.

5 Results

5.1 VCI

By analysing results from encroachment indicator calculation, the threshold for VCI is determined. In the three study areas 2162 cells where classified as *shrub and tree*. In Table 21 mean VCI, standard deviation 90th quantile for old and new ALS-data are given. Figure 21, Figure 22 and Figure 23 shows the corresponding histograms.

Table 21: VCI value in sample plots *shrub and tree encroachment*

	data old	data new	data old and new
Mean VCI	0.25	0.35	0.33
Standard deviation	0.12	0.19	0.18
90th quantile	0.42	0.61	0.59
Samples (n)	498	1665	2162

Old data: mean value for VCI in *shrub and tree* plots is 0.25, standard deviation 0.12. The 90th percentile is a VCI value of 0.42.
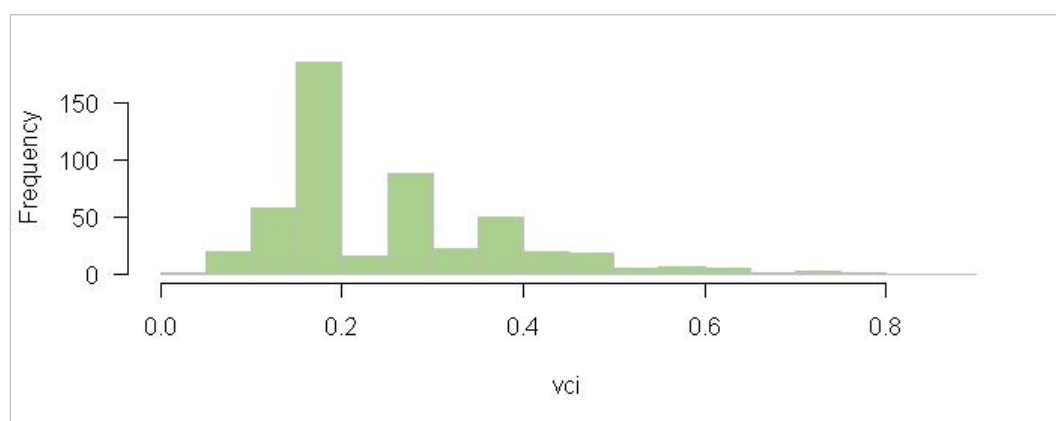
Figure 21: Histogram of VCI from classified new orthophoto sample plots, n = 498

New data: mean value for VCI in shrub and tree plots is 0.35, standard deviation 0.19. The 90th percentile is a VCI value of 0.61.
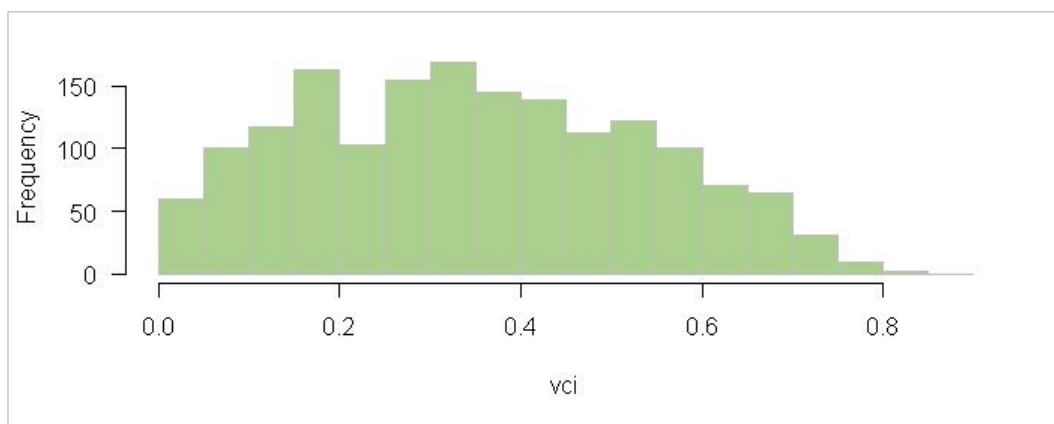
Figure 22: Histogram of VCI from classified new orthophoto sample plots, n = 1665

For old and new data, mean value for VCI in *shrub and tree* plots is 0.33, standard deviation 0.18. The 90th percentile is a VCI value of 0.59.
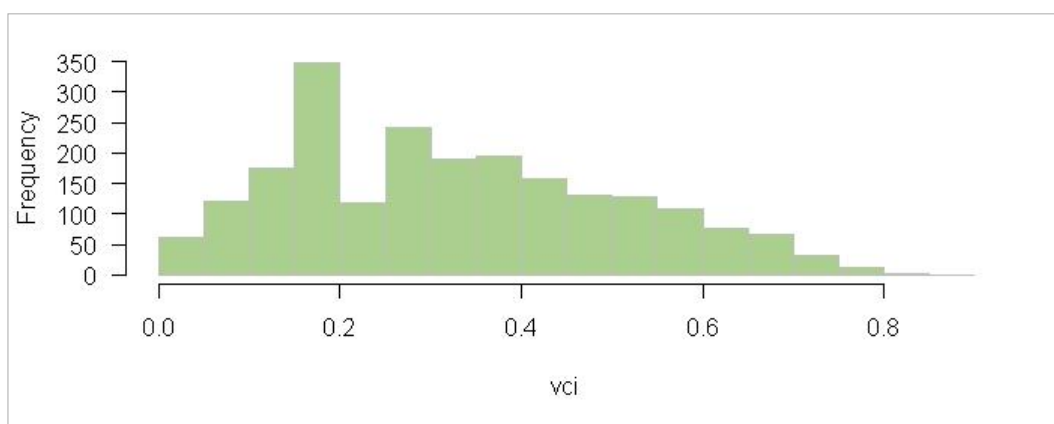
Figure 23: Histogram of VCI from classified old and new orthophoto sample plots, n = 2162

To identify the stem exclusion stage, examined by van Ewijk et al. (2011) with a mean VCI of 0.63, a threshold of maximum 0.61 is set for the encroachment indicator calculation.

5.2 Orthophoto Interpretation

The results of the orthophoto interpretation and indicator calculations for the three study areas are listed below. Each sample plot from a total of 450 randomly generated sample plots was assigned to one of the three categories *shrub and tree*, *other* or *unclassified*.

Saxeten

In the study area Saxeten 400 (old data) and 405 plots (new data) were classified as *shrub and tree* or *other*.

Table 22: Results Orthophoto interpretation Saxeten

Category	orthophoto old [n]	orthophoto old [%]	orthophoto new [n]	orthophoto new [n]
shrub and tree	78	17.1	94	20.7
other	322	70.8	311	68.4
unclassified	*55*	*12.1*	*50*	*11.0*
Plots classified (number and %)	400	100	405	100

Grandval

In the study area Grandval 394 (old data) and 397 plots (new data) were classified as *shrub and tree* or *other*.

Table 23: Results Orthophoto interpretation Grandval

Category	orthophoto old [n]	orthophoto old [%]	orthophoto new [n]	orthophoto new [n]
shrub and tree	8	1.8	33	7.3
other	386	85.8	364	80.9
unclassified	*39*	*8.6*	*53*	*11.8*
Plots classified (number and %)	394	100	397	100

Maienfeld

In the study area 442 (old data) and 447 plots (new data) were classified as *shrub and tree* or *other*.

Table 24: Results Orthophoto interpretation Maienfeld

Category	orthophoto old [n]	orthophoto old [%]	orthophoto new [n]	orthophoto new [n]
shrub and tree	30	6.7	54	12.0
other	412	91.6	393	87.3
unclassified	*8*	*1.8*	*3*	*0.7*
Plots classified (number and %)	442	100	447	100

5.3 Encroachment Indicator

The indicator calculation resulted in plots with shrub and tree encroachment and such without encroachment. To compare these results with the orthophoto interpretation, the class *unclassified* was excluded.

Saxeten

In Table 25 the achieved accuracies for the old data set and in Table 26 for the new data set are given.

Table 25: Accuracy assessment of the old data Saxeten

		classified (ALS data)			
		other (plots)	shrub and tree (plots)	Totals (plots)	User accuracy (%)
reference (orthophoto)	other (plots)	**299**	23	322	93
	shrub and tree (plots)	61	**17**	68	25
		360	40	**400**	
Producer's accuracy (%)		83	34		
Kappa: 0.29 n = 400					

Table 26: Accuracy assessment of the new data Saxeten

		classified (ALS data)			
		other (plots)	shrub and tree (plots)	Totals (plots)	User accuracy (%)
reference (orthophoto)	other (plots)	**266**	45	311	86
	shrub and tree (plots)	31	**63**	94	67
		297	108	**405**	
Producer's accuracy (%)		90	58		
Kappa: 0.55 n = 405					

Grandval

In Table 27 achieved accuracies for the old data set and in Table 28 for the new data set are given.

Table 27: Accuracy assessment of the old data Grandval

| | | classified (ALS data) | | | |
		other (plots)	shrub and tree (plots)	Totals (plots)	User accuracy (%)
reference (orthophoto)	'other' (plots)	**386**	8	394	98
	shrub and tree (plots)	11	**6**	17	35
		397	14	**411**	
Producer's accuracy (%)		97	43		
Kappa: 0.35 n = 400					

Table 28: Accuracy assessment of the new data Grandval

| | | classified (ALS data) | | | |
		other (plots)	shrub and tree (plots)	Totals (plots)	User accuracy (%)
reference (orthophoto)	other (plots)	**344**	20	364	95
	shrub and tree (plots)	7	**26**	33	79
		351	46	**397**	
Producer's accuracy (%)		98	57		
Kappa: 0.62 n = 397					

Maienfeld

In Table 29 the achieved accuracies for the old data set and in Table 30 for the new data set are given.

Table 29: Accuracy assessment of the old data Maienfeld

		classified (ALS data)			
		other (plots)	shrub and tree (plots)	Totals (plots)	User accuracy (%)
reference (orthophoto)	other (plots)	**407**	5	412	99
	shrub and tree (plots)	16	**14**	30	47
		423	19	**442**	
Producer's accuracy (%)		96	74		
Kappa: 0.55 n = 442					

Table 30: Accuracy assessment of the new data Maienfeld

		classified (ALS data)			
		'other' (plots)	shrub and tree (plots)	Totals (plots)	User accuracy (%)
reference (orthophoto)	other (plots)	**385**	8	393	98
	shrub and tree (plots)	23	**31**	54	57
		408	39	**447**	
Producer's accuracy (%)		94	79		
Kappa: 0.63 n = 442					

5.4 Overview

Table 31 summaries the results of the orthophoto interpretation. In all areas the percentage of encroachment increased between the old and the new data sets. Whereas plots of the category unclassified decreased in the study areas Saxeten and Maienfeld, they didn't in the study area Grandval.

Table 31: Comparison of Orthophoto interpretation

	Saxeten		Grandval		Maienfeld	
	old	new	old	new	old	new
year of orthophoto	2004	2012	2004	2012	2002	2014
category I *shrub and tree* [%]	17.1	20.7	1.8	7.3	6.7	12
category II *other* [%]	70.8	68.4	85.8	80.9	91.6	87.3
category III *unclassified* [%]	12.1	11	8.6	11.8	1.8	0.7
plots classified (category I and II) [n]	400	405	394	397	442	447

Table 32 shows the year of data collection and mean point density of ALS data.

Table 32: Summary of point density

Study area	Year of old data	mean density [p/m^2]	Year of new data	mean density [p/m^2]
Saxeten	2001	1.5	2012	18.9
Grandval	2001	1.2	2011	9.8
Maienfeld	2002	4.2	2015	21.7

Table 33 lists Cohen's kappa, producer's and overall accuracy for all examined data in the three study areas. Cohen's kappa ranges from 0.29 to 0.55 in the old data and from 0.55 to 0.63 in the new data.

Table 33: Comparison of Cohen's Kappa, producer's and overall accuracy

Study area	old data [Cohen's kappa]	Class *other* [%]	Class *shrub and tree* [%]	old data Overall accuracy [%]	new data [Cohen's kappa]	Class *other* [%]	Class *shrub and tree* [%]	new data Overall accuracy [%]
Saxeten	0.29	83	43	79	0.55	90	58	81
Grandval	0.35	97	43	95	0.62	98	57	93
Maienfeld	0.55	96	74	95	0.63	94	79	93

The producer's accuracy indicates the number of correctly classified samples using the indicator calculation. The accuracy for class *other* ranges from 83 to 98%, for both the old and new ALS data sets. For the class *shrub and tree*, accuracies between 34 and 74% for the old data set and between 57 and 79% for the new data set are obtained (Table 34).

Table 34: Comparison of producer's accuracies

Study area	old data other [%]	old data shrub an tree [%]	new data other [%]	new data shrub an tree [%]
Saxeten	83	34	90	58
Grandval	97	43	98	57
Maienfeld	96	74	94	79

6 Discussion

6.1 Encroachment Indicator

The thesis shows that the Vertical Complexity Index (VCI), implemented in the R-package lidR, in combination with the maximal Z value is suitable for the developed workflow. VCI was chosen due to the objective of using free or open source software for ALS processing. Without this limitation, maybe a modified workflow using a different software would have been implemented.

Producer's accuracies for the class *other* was only in one area smaller than 90% (old data Saxeten with 83%). For each study area, more than 300 plots were classified as *other* by the orthophoto interpretation. Regarding producer's accuracies for the class *shrub and tree* only for study area Maienfeld (old and new data) an accuracy of more than 70% were obtained. For the study area Grandval only eight plots (old data) respectively 33 plots (new data) were classified as *shrub and tree* by the orthophoto interpretation. Due to the fact that less samples led to more weight of an individual sample plot, errors for the indicator calculation were more effective. Consequently, lower producer's accuracies of 43% (old data), respectively 57% (new data) were obtained.

Table 35: Summary of point density, interpreted sample plots, producer's accuracy and Cohen's kappa

Study area	Year of ALS data	Mean density [p/m^2]	Interpreted sample plots Class *shrub and tree* [n]	Producer's accuracy Class *shrub and tree* [%]	Producer's accuracy Class *other* [%]	Cohen's kappa
Grandval	2001	1.2	14	43	97	0.35
Saxeten	2001	1.5	40	43	83	0.29
Maienfeld	2002	4.2	19	74	96	0.55
Grandval	2011	9.8	46	57	98	0.62
Saxeten	2012	18.9	108	58	90	0.55
Maienfeld	2015	21.7	39	79	94	0.63

Congalton (1991) recommends classifying at least 50 samples per class. This '*rule of thumb*' has not been considered in the sample design used in this thesis. Otherwise, a stratified random sampling with at least 50 sample plots per class could have been implemented.

As shown in Table 35 only in the new data set for the study area Saxeten more than 50 sample plots were classified as *shrub and tree*. Due to amount of sample plots classified as *others* overall accuracies, which range between 79 and 95% for all study areas, must be interpreted carefully.

The interpretation of Kappa results turned out to be difficult. On one hand, Kappa used as an index for remote sensing assessment is a controversial issue and on the other hand, comparable studies are rare. Table 35 gives an overview of obtained Cohen's Kappa, producer's and overall accuracy.

Apart from the old data from Saxeten (Kappa = 0.29) and Grandval (Kappa = 0.35), the other data sets in the three study areas achieved a Kappa of 0.55 or higher. Due to Schaepman et al. (2015) there is no universal interpretation of Kappa values. Nevertheless, values between 0.41 and 0.60 in general are interpreted as values with a moderate, and values from 0.61 to 0.80 as values with a good agreement to the reference.

6.2 Orthophoto Interpretation

For all three study areas, the number of sample plots classified as *shrub and tree* increased from the old to the new image. Furthermore, for all study areas total number of plots classified were stable between the two ALS data sets. Overall for 9 % of sample plots an interpretation was not possible due to shadows large trees or the topography.

The orthophoto interpretation was not verified by ground truth data, as for a comparison of the two remote sensing techniques the accuracy can be regarded as sufficient. Potential sources of errors include the omission of small trees in pastures due to small spectral differences in the imagery and the detection of high vegetation as encroachment due to misinterpretation of height.

6.3   Software and Workflow

To familiarise oneself with the use of ALS processing software required more time than initially expected. All tools were appropriate regarding their purpose in the workflow and turned out to be robust, also for large datasets.

In order to reduce computation time, the classes forest, roads, buildings, rock and others from land use dataset (cadastral survey) were excluded from VCI and maximum Z value calculation. This step can be time consuming depending on the area of interest and data availability from the cadastral survey. Regarding the implementation of writing results of calculations directly to a PostgreSQL database (Table 37), the author suggests to calculate the VCI and maximum Z value area-wide for further analysis. Exclusion of area of non-interest can be done easier afterwards in PostGIS.

The direct implementation of the indicator calculation in PDAL or LAStools may be faster than the combination of PDAL, R and PostgreSQL/PostGIS. Currently, LAStools offers the possibility[25] to calculate vegetation cover. When executing this calculation for each single height bin, the VCI could be calculated with a few intermediate step in the tool lascanopy (not free to use, compare chapter 2.2).

6.4   Minimal Point Density

A minimal point density of ALS data to obtain a reasonable detection rate is not derivable from the results. Study area specific difficulties and different sources of errors may have more impact than the point density (see chapter 6.5). The two lowest producer's accuracies are obtained from ALS data with low point density of 1.2, respectively 1.5 points/m^2 (Table 35). In contrast with a point density of 4.2 points/m^2 in the study area Maienfeld a producer's accuracy of 74% is reached.

---

[25] https://groups.google.com/forum/#!topic/lastools/nEYDRc5jdu8 (visited 01.10.2017)

6.5 Study Area Characteristics

Grandval

Wooded pastures (pastures with high density of trees) and stonewalls that border these pastures are typical for the Jura region. Such specific elements resulted in an erroneous positive shrub and tree encroachment indicator (Figure 24 and Figure 25). Moreover, for the orthophoto interpretation tree shadows were the main reason for the relatively high number of unclassified sample plots.
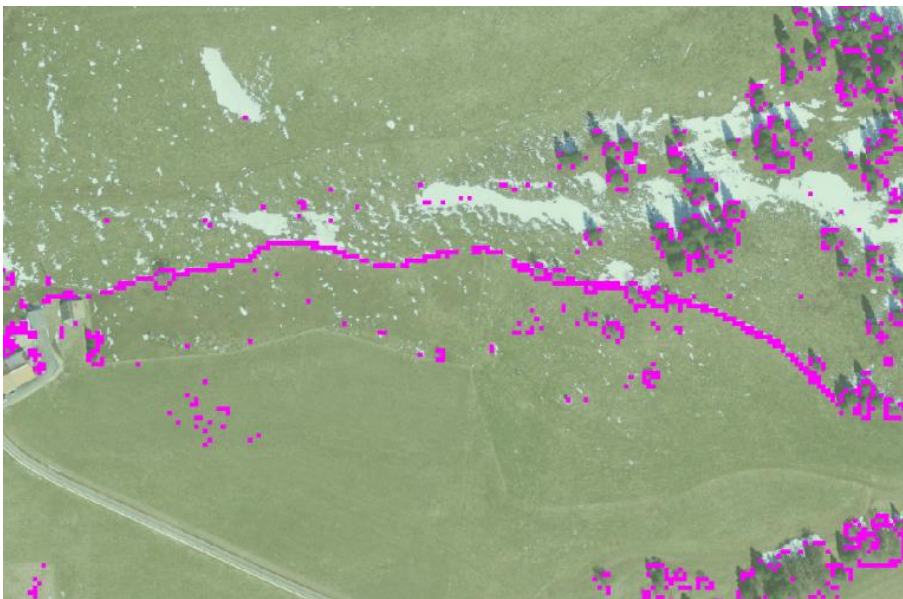
Figure 24: The linear element in the centre is a typical stonewall of Jura region (false positive)

Figure 25: High density of trees in pasture in Jura region

Saxeten

The rocky area of Saxeten is characterized by steep relief with large shadows in the orthophotos that resulted in many unclassified sample plots (example in Figure 26).

Figure 26: Shadows caused by topography in Saxeten

Maienfeld

Since a technical border, that involves parts of four communes as shown in Figure 13, defines the study area Maienfeld, additional work to collect the data from the cadastral survey was required. Roads and settlements are less present compared to the entire area of the commune or to the two other study areas. However, this did not affect the workflow. The new ALS data from 2015 has been collected in August of that year under leaf-on conditions. Depending on use of the pastures, e.g. as grazing or hay meadow, grass vegetation may still be high in August. Thus, small shrubs and trees might very likely not be detected.

7 Conclusion

LiDAR data contains numerous information and provides manifold possibilities for the analysis of landscape and particularly of vegetation. This thesis showed, that it is possible to assign shrub and tree encroachment in alpine pastures in Switzerland from ALS data with middle to high point density.

By extending the Vertical Complexity Index (VCI) with a maximum Z value, a stable shrub and tree encroachment indicator for alpine regions was calculated. In Maienfeld, one of the three study areas, for both the old and new ALS data sets, data with middle to high point density was available. This good data quality led to the following results: for the classification category *shrub and tree encroachment* an accuracy of 74% (ALS data 2002, 4.2 points/m^2) and 79% (ALS data 2015, 21.7 points/m^2) was achieved. A minimal point density could not be determined.

In the Jura region, traditional wooded pastures led to elevated false positive sample plots.

The used software PDAL, R and PostgreSQL/POSTGIS in the implemented workflow was practical and stable for processing and analysing the ALS data.

8 Outlook

Overall, the approach to detect shrub and tree encroachment as developed in this thesis is relevant for practical application. It can easily be implemented into projects and applied to larger areas.

The projected data availability of ALS data in the next 6 years (Bundesamt für Landestopographie swisstopo, 2017) will be an excellent basis for further studies related to shrub and tree encroachment.

From a technical point of view, pulses with certain scan angles off-nadir could be excluded from analysis from ALS data with higher density. Thus, more accurate and precise results for areas like e.g. Grandval with a dominance of traditional wooded pastures, might be obtained.

The achieved accuracies for the encroachment indicator may be a solid basis for discussing areas of priority. In particular, aggregation of small encroachment patches and visualisation over large areas can assist decision makers in prioritising intervention areas.

Furthermore, analysing full waveform ALS data as provided by swisstopo in the next years, is promising regarding an extension of vegetation detection and classification.

9 List of References

AGRIDEA 2015. Verbuschung und Problempflanzen im Sömmerungsgebiet, Leitfaden für Kontrollierende.

ALEXANDER, C., DEÁK, B., KANIA, A., MÜCKE, W. & HEILMEIER, H. 2015. Classification of vegetation in an open landscape using full-waveform airborne laser scanner data. *International Journal of Applied Earth Observation and Geoinformation,* 41**,** 76-87.

AMT FÜR WALD DES KANTONS BERN 2014. LIDAR-Daten Kanton Bern.

ANADÓN, J. D., SALA, O. E., TURNER, B. & BENNETT, E. M. 2014. Effect of woody-plant encroachment on livestock production in North and South America. *Proceedings of the National Academy of Sciences,* 111**,** 12948-12953.

ANDERSON, K., HANCOCK, S., DISNEY, M. & GASTON, K. J. 2016. Is waveform worth it? A comparison of LiDAR approaches for vegetation and landscape characterization. *Remote Sensing in Ecology and Conservation,* 2**,** 5-15.

ASPRS 2013. LAS SPECIFICATION VERSION 1.4 – R13 15 July 2013. *American Society for Photogrammetry & Remote Sensing*.

BALENOVIĆ, I., ALBERTI, G. & MARJANOVIĆ, H. 2013. Airborne Laser Scanning-the Status and Perspectives for the Application in the South-East European Forestry. *South-east European forestry,* 4**,** 59-79.

BATTAGLINI, L., BOVOLENTA, S., GUSMEROLI, F., SALVADOR, S. & STURARO, E. 2014. Environmental sustainability of Alpine livestock farms. *Italian Journal of Animal Science,* 13**,** 3155.

BAUR, P., MÜLLER, P. & HERZOG, F. 2007. Alpweiden im Wandel. *Agrarforschung,* 14**,** 254-259.

BLASCHKE, T. 2010. Object based image analysis for remote sensing. *ISPRS journal of photogrammetry and remote sensing,* 65**,** 2-16.

BLASCHKE, T., TIEDE, D. & HEURICH, M. 2004. 3D landscape metrics to modelling forest structure and diversity based on laser scanning data. *International Archives of the Photogrammetry, Remote Sensing and Spatial Information Sciences,* 36**,** 129-132.

BOLLMANN, R., SCHNEIDER, M. & FLURY, C. 2014. Minimalnutzungsverfahren zur Offenhaltung der Kulturlandschaft. *Agroscope Science*.

BRÄNDLI, U., CIOLDI, F., FISCHER, C., HEROLD-BONARDI, A., KELLER, H. & MEILE, R. 2014. Viertes Schweizerisches Landesforstinventar-Ergebnistabellen und Karten im Internet zum LFI 2009-2013 (LFI4b). Birmensdorf, Eidg. Forschungsanstalt WSL.

BRASSEL, P. L., H 2001. Swiss National Forest Inventory: Methods and Models of the Second Assessment. *Birmensdorf, Swiss Federal Research Institute WSL***,** 336.

BRUGGISSER, M., RONCAT, A., SCHAEPMAN, M. E. & MORSDORF, F. 2017. Retrieval of higher order statistical moments from full-waveform LiDAR data for tree species classification. *Remote Sensing of Environment,* 196**,** 28-41.

BUNDESAMT FÜR LANDESTOPOGRAPHIE SWISSTOPO 2008. Alte SWISSIMAGE Farborthophotos - Übersichten der verfügbaren Bilder (pro Jahr).

BUNDESAMT FÜR LANDESTOPOGRAPHIE SWISSTOPO 2010a. Die LiDAR Messkampagne und LiDAR-Daten der swisstopo.

BUNDESAMT FÜR LANDESTOPOGRAPHIE SWISSTOPO 2010b. SWISSIMAGE - Das digital Farborthophotomosaik der Schweiz.

BUNDESAMT FÜR LANDESTOPOGRAPHIE SWISSTOPO. 2016. *Height Model swissALTI3D* [Online]. http://www.swisstopo.admin.ch/internet/swisstopo/en/home/products/height/swissALTI3D.html: Federal Office of Topography swisstopo. [Accessed 2016-06-21].

BUNDESAMT FÜR LANDESTOPOGRAPHIE SWISSTOPO. 2017. *Beschaffung von LiDAR-Daten* [Online]. Wabern b. Bern. Available: {Bundesamt für Landestopographie swisstopo, 2015 #36} [Accessed 09.10 2017].

BUNDESAMT FÜR LANDWIRTSCHAFT BLW 2016. Agrarbericht 2016.

BUNDESAMT FÜR LANDWIRTSCHAFT BLW 2017. Landwirtschaftliche Zonen-Verordnung; SR 912.1, Weisungen und Erläuterungen.

BUNDESAMT FÜR STATISTIK BFS, GEOSTAT 2014. Arealstatistik nach Nomenklatur 2004 – Bodenbedeckung. https://www.bfs.admin.ch/bfs/de/home/statistiken/raum-umwelt/nomenklaturen/arealstatistik/nolc2004.assetdetail.313706.html.

BUNDESAMT FÜR STATISTIK BFS, GEOSTAT 2016. Arealstatistik nach Nomenklatur 2004 – Standard. https://www.bfs.admin.ch/bfs/de/home/statistiken/raum-umwelt/nomenklaturen/arealstatistik/noas2004.assetdetail.264654.html.

BUTLER, H. & GERLEK, M. 2017. PDAL - Point Data Abstraction Library.

CALDWELL, J. 2013. *LiDAR - Best Practice* [Online]. http://eijournal.com/print/articles/lidar-best-practices: Earth Imaging Journal. [Accessed 2016-06-21].

CAO, L., COOPS, N. C., INNES, J. L., DAI, J., RUAN, H. & SHE, G. 2016. Tree species classification in subtropical forests using small-footprint full-waveform LiDAR data. *International Journal of Applied Earth Observation and Geoinformation,* 49**,** 39-51.

COHEN, J. 1960. A coefficient of agreement for nominal scales. *Educational and Psychological Measurement*.

CONGALTON, R. G. 1991. A review of assessing the accuracy of classifications of remotely sensed data. *Remote sensing of environment,* 37**,** 35-46.

ELDRIDGE, D. J., BOWKER, M. A., MAESTRE, F. T., ROGER, E., REYNOLDS, J. F. & WHITFORD, W. G. 2011. Impacts of shrub encroachment on ecosystem structure and functioning: towards a global synthesis. *Ecology Letters,* 14**,** 709-722.

ESPOSITO, G., MASTROROCCO, G., SALVINI, R., OLIVETI, M. & STARITA, P. 2017. Application of UAV photogrammetry for the multi-temporal estimation of surface extent and volumetric excavation in the Sa Pigada Bianca open-pit mine, Sardinia, Italy. *Environmental Earth Sciences,* 76**,** 103.

FLURY, C., HUBER, R. & TASSER, E. 2013. Future of mountain agriculture in the Alps. *The Future of Mountain Agriculture.* Springer.

FOODY, G. M. 2009. Sample size determination for image classification accuracy assessment and comparison. *International Journal of Remote Sensing,* 30**,** 5273-5291.

GINZLER, C. 2016. LiDAR availability 2015. *CAS Vegetationsanalyse & Feldbotanik - GIS und Fernerkundung (unpublished),* WSL.

GINZLER, C. & WASER, L. T. 2017. Entwicklungen im Bereich der Fernerkundung für forstliche Anwendungen. *Schweizerische Zeitschrift fur Forstwesen,* 168**,** 118-126.

GONSETH, Y., WOHLGEMUTH, T., SANSONNES, B. & BUTTLER, A. 2001. Die biogeographischen Regionen der Schweiz. Erläuterungen und Einteilungsstandard. *Umwelt Materialien, Bundesamt für Umwelt, Wald und Landschaft Bern.,* Nr. 137 48.

HEDINGER, C. U. B. 2014. Artenreiche Grün- und Streueflächen im Sömmerungsgebiet. *Agridea*

HEIPKE, C. 2017. Photogrammetrie und Fernerkundung–eine Einführung. *Photogrammetrie und Fernerkundung.* Springer.

HELLESEN, T. & MATIKAINEN, L. 2013. An object-based approach for mapping shrub and tree cover on grassland habitats by use of LiDAR and CIR orthoimages. *Remote Sensing,* 5**,** 558-583.

HOFMANN, P. 2015. Digital image analysis - classification methods (unpublished). *Module Remote Sensing, Handout Lesson 8.* Department of Geoinformatics - Z_GIS / University of Salzburg.

HOLZER, K. 1967. Das Wachstum des Baumes in seiner Anpassung an zunehmende Seehöhe. *Mitt. Forstl. Bundesversuchsanst. Wien,* 75**,** 427-456.

HUNZIKER, M. 2012. Die Bedeutungen der Landschaft für den Menschen: objektive Eigenschaft der Landschaft oder individuelle Wahrnehmung des Menschen? *Landnutzungswandel in Mitteleuropa***,** 63.

HYYPPÄ, J., HYYPPÄ, H., YU, X., KAARTINEN, H., KUKKO, H. & HOLOPAINEN, M. 2009. Forest inventory using small-footprint airborne lidar. *Topographic laser ranging and scanning: principles and processing. CRC Press, Taylor & Francis London***,** 335-370.

ISENBURG, M. 2017. LAStools - efficient tools for LiDAR processing. Version 170628. https://rapidlasso.com/.

KARAN, E. P., SIVAKUMAR, R., IRIZARRY, J. & GUHATHAKURTA, S. 2013. Digital modeling of construction site terrain using remotely sensed data and geographic information systems analyses. *Journal of Construction Engineering and Management,* 140**,** 04013067.

KOCH, B. & SCHMID, S. 2013. Wertvolle Artenvielfalt in Grasland von verbuschten Alpweiden. *AGRAR FORSCHUNG SCHWEIZ***,** 172.

KOLECKA, N., KOZAK, J., KAIM, D., DOBOSZ, M., GINZLER, C. & PSOMAS, A. 2015. Mapping secondary forest succession on abandoned agricultural land with LiDAR point clouds and terrestrial photography. *Remote Sensing,* 7**,** 8300-8322.

LAUBER, S., HERZOG, F., SEIDL, I., BÖNI, R., BÜRGI, M., GMÜR, P., HOFER, G., MANN, S., RAAFLAUB, M. & SCHICK, M. 2013. Zukunft der Schweizer Alpwirtschaft. *Fakten, Analysen und Denkanstösse aus dem Forschungsprogramm AlpFUTUR. Eidgenössische Forschungsanstalt für Wald, Schnee und Landschaft WSL, Birmensdorf.*

LILLESAND, T., KIEFER, R. W. & CHIPMAN, J. 2014. *Remote sensing and image interpretation*, John Wiley & Sons.

MACDONALD, D., CRABTREE, J., WIESINGER, G., DAX, T., STAMOU, N., FLEURY, P., LAZPITA, J. G. & GIBON, A. 2000. Agricultural abandonment in mountain areas of Europe: environmental consequences and policy response. *Journal of environmental management,* 59**,** 47-69.

MACK, G., WALTER, T. & FLURY, C. 2013. Seasonal alpine grazing trends in Switzerland: economic importance and impact on biotic communities. *Environmental science & policy,* 32**,** 48-57.

MANDLBURGER, G. 2017. Bathymetry from active and passive airborne remote sensing–looking back and ahead.

MCC. NETTING, R. 1972. Of men and meadows: strategies of Alpine land use. *Anthropological Quarterly*, 132-144.

MCGILL, M. J. 2003. *Encyclopedia of Optical Engineering: Las-Pho, pages 1114-1127*, CRC press.

MONGUS, D. & ŽALIK, B. 2015. An efficient approach to 3D single tree-crown delineation in LiDAR data. *ISPRS Journal of Photogrammetry and Remote Sensing,* 108**,** 219-233.

PENNER, M., WOODS, M. & PITT, D. G. 2015. A comparison of airborne laser scanning and image point cloud derived tree size class distribution models in boreal Ontario. *Forests,* 6**,** 4034-4054.

PONTIUS JR, R. G. & MILLONES, M. 2011. Death to Kappa: birth of quantity disagreement and allocation disagreement for accuracy assessment. *International Journal of Remote Sensing,* 32**,** 4407-4429.

POSTGRESQL GLOBAL DEVELOPMENT GROUP 2017. PostgreSQL. 9.5.7 ed.: PostgreSQL Global Development Group.

QGIS DEVELOPMENT TEAM 2017. QGIS Geographic Information System. 2.14.19-Essen ed.: Open Source Geospatial Foundation.

R DEVELOPMENT CORE TEAM 2017. R: A language and environment for statistical computing. Vienna, Austria: R Foundation for Statistical Computing.

REFRACTIONS RESEARCH, PAUL RAMSEY, DAVE BLASBY, KEVIN NEUFELD, MARK CAVE-AYLAND, REGINA OBE, SANDRO SANTILLI, OLIVIER COURTIN, NICKLAS AVÉN, BBORIE PARK, PIERRE RACINE, JEFF LOUNSBURY, CHRIS HODGSON, JORGE ARÉVALO, MATEUSZ LOSKOT, NORMAN VINE, CARL ANDERSON, RALPH MASON, KLAUS FOERSTER, BRUNO WOLFF III & MARKUS SCHABER 2017. PostGIS. 2.2.1 ed.: Refractions Research.

ROUSSEL, J.-R. 2017. Package 'lidR': Airborne LiDAR Data Manipulation and Visualization for Forestry Applications. 1.2.0 ed.

SAHARA, E. A., SARR, D. A., VAN KIRK, R. W. & JULES, E. S. 2015. Quantifying habitat loss: Assessing tree encroachment into a serpentine savanna using dendroecology and remote sensing. *Forest Ecology and Management,* 340**,** 9-21.

SCHAEPMAN, M. E., DE JONG, R. & LEITERER, R. 2015. Grundlagen Fernerkundung -12 Image classification (Department of Geography / Unveristy of Zurich UZH). http://www.geo.uzh.ch/microsite/rsl-documents/teaching/BSc/geo123/2015/GEO123.1_Lecture_12_FS2015_ImageClassification_v2_dpi220.pdf.

SCHWEIZERISCHER BUNDESRAT 2013. Verordnung über die Direktzahlungen an die Landwirtschaft (Direktzahlungsverordnung, DZV) vom 23. Oktober 2013. http://www.blw.admin.ch/themen/00005/00044/01178/01689/index.html?lang=de.

SHANNON, C. E. 1948. The mathematical theory of communication. *Bell System Technical Journal,* 27**,** 379-423 and 623-656.

SILVA, C. A., CROOKSTON, N. L., T, H. A. & VIERLING, L. A. 2015. Package 'rLiDAR': LiDAR Data Processing and Visualization. 0.1 ed.

SUTTER, R. 2007. Erosion im Alpgebiet Schlussbericht. *Agricultura Ingenieurbüro, Appenzell*.

VAN EWIJK, K. Y., TREITZ, P. M. & SCOTT, N. A. 2011. Characterizing forest succession in Central Ontario using LiDAR-derived indices. *Photogrammetric Engineering & Remote Sensing,* 77**,** 261-269.

WANG, Z., GINZLER, C. & WASER, L. T. 2015. A novel method to assess short-term forest cover changes based on digital surface models from image-based point clouds. *Forestry: An International Journal of Forest Research,* 88**,** 429-440.

WASER, L., BALTSAVIAS, E., ECKER, K., EISENBEISS, H., FELDMEYER-CHRISTE, E., GINZLER, C., KÜCHLER, M. & ZHANG, L. 2008. Assessing changes of forest area and shrub encroachment in a mire ecosystem using digital surface models and CIR aerial images. *Remote Sensing of Environment,* 112**,** 1956-1968.

WU, Z., DYE, D., STOKER, J., VOGEL, J., VELASCO, M. & MIDDLETON, B. 2016. Evaluating Lidar Point Densities for Effective Estimation of Aboveground Biomass. *International Journal of Advanced Remote Sensing and GIS***,** pp. 1483-1499.

ZOLLER, H. & BISCHOF, N. 1980. Stufen der Kulturintensität und ihr Einfluss auf Artenzahl und Artengefüge der Vegetation. *Phytocoenologia***,** 35-51.

10 Appendix

A) Overview selection criteria by canton

Table 36: Selection criteria by canton

Canton	Area [km²]	Flight year swisstopo	Flight year canton	Density [p/m²]	Biogeographic region (number of region)	encroachment points	Mean encroachment [points per km²]
GR	7105	2003	2015 (partially by WSL)	> 18	3 / 5 / 6	2157	0.3
VS	5224	2001, (2002), 2005	-	-	4	1957	0.37
TI	2812	(2003), 2005	-	-	6	1358	0.48
BE	5959	2000-2002 (2005)	2011 - 2013	4 - 8	1 / 2 / 3	1255	0.21
VD	3212	2001	2015	10 - 15	1 / 2 / 3	1049	0.33
SG	2026	2002, 2003	-	-	2 / 3	514	0.25
FR	1671	2000, 2001	-	-	2 / 3	367	0.22
SZ	908	2002	-	-	2 / 3	221	0.24
GL	685	2002	2012		3	204	0.3
LU	1493	2000-2002	2012 (partially)	5	2 / 3	199	0.13
UR	1077	2002, 2003	-	-	3 / 5	188	0.17
OW	491	2002- 2007	-	-	3	165	0.34
NE	803	2000, 2001	2010	7	1 / 2	136	0.17
ZH	1729	2001, 2002	2014	8	2 / 3	129	0.07
TG	991	2002	2014	8	2	123	0.12
AG	1404	2001, 2002	2013	5 - 7	1 / 2	86	0.06
JU	839	2001, 2006, 2007	2006-2007		1	77	0.09
NW	276	2002 - 2007	-	-	3	64	0.23
AR	243	2002	2014	19.35	2 / 3	62	0.26
SO	791	2000, 2001	2014	4	1 / 2	59	0.07
GE	16	2001, 2005	-	-	2	41	0.15
BL	518	2001, 2007	2012	7	1 / 2	37	0.07
AI	173	2002	-	-	3	36	0.21
SH	298	2002	2013	5	1 / 2	33	0.11
ZG	239	2002	2012 - 2013	4	2 / 3	17	0.07
BS	37	2007	2012		2	1	0.03

B) Improved workflow, writing data to PostgreSQL table from R

Table 37: Example workflow, writing data to PostgreSQL

```
library(data.table)
library(RPostgreSQL)
library(lidR)
pw <- {"password"}
drv <- dbDriver("PostgreSQL")
con <- dbConnect(drv, dbname = "dbname", host = "host", port = 5432, user = "user", password = pw)
dbExistsTable(con, c("master","mf_vci02"))
startingDir <- "E:/Geodaten/lidar_mt/maienfeld/2002/norm"
lasFiles <- list.files(startingDir, pattern = ".laz", full.names = TRUE)
for (fileName in lasFiles) {
  las = readLAS(fileName)
  vci = las %>% grid_metrics(VCI(Z, by=1, zmax = 40), res = 3)
  vci2 <- data.table(vci)[, .(X, Y,V1)]
  names(vci2)[names(vci2)=="X"] <-"x"
  names(vci2)[names(vci2)=="Y"] <-"y"
  names(vci2)[names(vci2)=="V1"] <-"vci"
  dbWriteTable(con, c("master","mf_vci02"), value=vci2, append=TRUE, row.names = FALSE)}
```

C) Generalization of data for further analysis and presentation CODE

For further analysis and for evaluate areas priority, encroachment indicator is converted to polygons. Therefore, the area of clustered encroachment points can be calculated and visualized.

Table 38: Cluster point data and convert in polygon in PostGIS

```sql
CREATE OR REPLACE FUNCTION master.funct_clust(
    name character varying,
    geom character varying,
    gid character varying,
    radius numeric)
  RETURNS SETOF record AS
$BODY$
DECLARE
    lid_new    integer;
    dm_nr      integer := 1;
    outr       record;
    innr       record;
    r          record;
BEGIN

    DROP TABLE IF EXISTS master.tmp;
    EXECUTE 'CREATE TEMPORARY TABLE master.master.tmp AS SELECT '||gid||', '||geom||' FROM '||name;
    ALTER TABLE master.tmp ADD COLUMN dmn integer;
    ALTER TABLE master.tmp ADD COLUMN chk boolean DEFAULT FALSE;
    EXECUTE 'UPDATE master.tmp SET dmn = '||dm_nr||', chk = FALSE WHERE '||gid||' = (SELECT MIN('||gid||')
FROM master.tmp)';

    LOOP
      LOOP
        FOR outr IN EXECUTE 'SELECT '||gid||' AS gid, '||geom||' AS geom FROM master.tmp WHERE dmn =
'||dm_nr||' AND NOT chk' LOOP
          FOR innr IN EXECUTE 'SELECT '||gid||' AS gid, '||geom||' AS geom FROM master.tmp WHERE dmn IS NULL'
LOOP
            IF ST_DWithin(outr.geom, innr.geom, radius) THEN
            --IF ST_DWithin(outr.geom, innr.geom, radius) THEN
              EXECUTE 'UPDATE master.tmp SET dmn = '||dm_nr||', chk = FALSE WHERE '||gid||' = '||innr.gid;
            END IF;
          END LOOP;
          EXECUTE 'UPDATE master.tmp SET chk = TRUE WHERE '||gid||' = '||outr.gid;
        END LOOP;
        SELECT INTO r dmn FROM master.tmp WHERE dmn = dm_nr AND NOT chk LIMIT 1;
        EXIT WHEN NOT FOUND;
      END LOOP;
      SELECT INTO r dmn FROM master.tmp WHERE dmn IS NULL LIMIT 1;
      IF FOUND THEN
        dm_nr := dm_nr + 1;
```

```
        EXECUTE 'UPDATE master.tmp SET dmn = '||dm_nr||', chk = FALSE WHERE '||gid||' = (SELECT MIN('||gid||')
FROM master.tmp WHERE dmn IS NULL LIMIT 1)';
    ELSE
        EXIT;
    END IF;
  END LOOP;

  RETURN QUERY EXECUTE 'SELECT ST_ConvexHull(ST_Collect('||geom||')) FROM master.tmp GROUP by dmn';

  RETURN;
END
$BODY$
  LANGUAGE plpgsql VOLATILE
  COST 100
  ROWS 1000;
ALTER FUNCTION master. funct_clust (character varying, character varying, character varying, numeric)
```

Source, adapted from https://gis.stackexchange.com/questions/11567/spatial-clustering-with-postgis

Table 39: Generalization and smoothing of clustered data in PostGIS

```
CREATE TABLE master.poly AS SELECT * FROM funct_clust('master.index15', 'geom', 'gid', 4.5) AS g(geom
geometry);

## Add column with area
ALTER TABLE master.poly ADD AREA INTEGER;
UPDATE master.poly SET area = ST_Area(geom);
UPDATE master.poly SET geom = (SELECT ST_Buffer(geom,5.5));

CREATE TABLE master.poly2 AS SELECT (ST_Dump(singlegeom)).geom
FROM (
  SELECT ST_Multi(ST_Union(poly.geom)) as singlegeom
  FROM master.poly) AS p;
ALTER TABLE master.poly2 ADD AREA INTEGER;
UPDATE master.poly2 SET area = ST_Area(geom);
ALTER TABLE master.poly2 ADD GID SERIAL;
ALTER TABLE master.poly2 ADD PRIMARY KEY(gid);

## delete holes in polygons
UPDATE master.poly2 p
SET geom = a.geom
FROM (
  SELECT gid, ST_Collect(ST_MakePolygon(geom)) AS geom
  FROM (
    SELECT gid, ST_NRings(geom) AS nrings,
      ST_ExteriorRing((ST_Dump(geom)).geom) AS geom
    FROM master.poly2
    WHERE ST_NRings(geom) > 1
    ) s
```

```
    GROUP BY gid, nrings
    HAVING nrings > COUNT(gid)
    ) a
WHERE p.gid = a.gid;

##smooth outline with buffer
UPDATE master.poly2 SET geom = (SELECT ST_Buffer(geom,-4));
UPDATE master.poly2 SET geom = (SELECT ST_Buffer(geom,1));
UPDATE master.poly2 SET geom = (SELECT ST_Buffer(geom,-2));
UPDATE master.poly2 SET geom = (SELECT ST_Buffer(geom,1));

## explode multipolygon, delete small patches
CREATE TABLE master.poly3 AS
    SELECT gid, area, (ST_DUMP(geom)).geom::geometry(Polygon,21781) AS geom FROM master.poly2;
UPDATE master.poly3 SET area = ST_Area(geom);
DELETE FROM master.poly3 WHERE area<100;
```

**D) Generalization of data for further analysis and presentation
EXAMPLE MAP**

Figure 27: example of area with indicator values as encroachment points

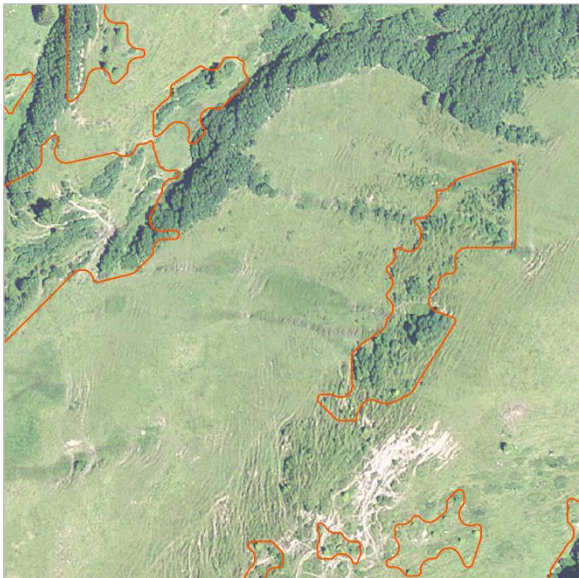Figure 28: example area with summarized encroachment area as polygon

Figure 29: example area with summarized encroachment area as polygon, orthophoto